THE ASTROPHYSICAL JOURNAL, 347:29–51, 1989 December 1

CONTINUUM ENERGY DISTRIBUTIONS OF QUASARS: SHAPES AND ORIGINS

D. B. SANDERS, E. S. PHINNEY,[1] G. NEUGEBAUER, B. T. SOIFER, AND K. MATTHEWS
Palomar Observatory, California Institute of Technology
Received 1989 February 2; accepted 1989 June 2

ABSTRACT

Continuum observations from ~0.3 nm to 6 cm ($10^{9.7}$–10^{18} Hz) are presented for 109 bright quasars from the Palomar-Green (PG) survey. Two-thirds of the quasars have been detected in the infrared at wavelengths between 10 and 100 μm. All of the PG quasars appear to emit the bulk of their luminosity (typically more than 90%) between 3 nm and 300 μm (10^{12}–10^{17} Hz). The total luminosity at wavelengths longer than 1 μm is typically 20%–40% of that at wavelengths shortward of 1 μm.

The gross shape of the energy distributions between 3 nm and 300 μm is remarkably similar for all the quasars except the flat-spectrum radio-loud quasars like 3C 273 and can plausibly be fitted by two broad components of thermal emission. In this interpretation the emission in the spectral range ~10 nm to 0.3 μm, the "big blue bump," is dominated by 10,000–100,000 K thermal emission from an accretion disk. The emission between 2 μm and 1 mm, the "infrared bump," is made up of reradiation from dust in a distorted disk extending from 0.1 pc to more than 1 kpc. The fairly small range in the relative sizes of the bumps suggests that the covering factor in most of the PG quasars is similar. There is no obvious connection between the strengths of the blue and infrared peaks and whether or not the quasar is radio quiet or radio loud. The mass of infrared emitting dust is estimated to be ~0.01 $M_\odot$ at 2 μm and ~10^5 $M_\odot$ at 60 μm. The radiation from 0.5 μm is thermal emission from the portion of the disk between 0.1 and 1 pc, illuminated primarily by the clouds of the broad-line region. The radiation from 5 μm to 1 mm is reradiation from a warped disk at distances greater than 1 pc from the central source, which is heated directly by radiation from the central source. Optically thin atomic emission (free-free and partially thermalized lines and bound-free) from gas within 1 pc of the central source, whose dust has sublimated, probably contributes to the flux from 0.5 to 2 μm. We believe that there is no convincing evidence for energetically significant nonthermal radiation in the wavelength range 3 nm to 300 μm in the continua of the radio-quiet and steep-spectrum radio-loud PG quasars.

Subject headings: quasars — radiation mechanisms — spectrophotometry

I. INTRODUCTION

Satellite observations in the infrared, ultraviolet, and X-ray bands have made it possible to study the continuum emission of quasars over a very broad range of frequencies. Coupled with sensitive new millimeter wave and radio observations, the satellite observations make it possible to present a fairly complete picture of the continuum energy distributions of both radio loud and radio quiet quasars over the eight decade wavelength range from ~0.3 nm to 6 cm ($10^{9.7}$–10^{18} Hz). A sample of quasars that has proven to be accessible to studies at a variety of wavelengths is the Palomar bright quasar survey (BQS) of Schmidt and Green (1983). The BQS is a statistically complete sample of over 100 of the brightest quasars found in the Palomar-Green (PG) survey of stellar objects with ultraviolet excess (Green, Schmidt, and Liebert 1986).

A major gap in the knowledge of the far-infrared properties of quasars was closed by the *Infrared Astronomical Satellite* (*IRAS*) which was sensitive enough to detect many of the brightest quasars. Initial observations of quasars from *IRAS* have been presented by Neugebauer *et al.* (1986), including measurements of 32 PG quasars. In this paper, *IRAS* observations, either detections or limits, are presented for the remainder of the PG quasars. In addition, new measurements at 10 μm from the Palomar 5 m telescope are presented; the number of PG quasars now detected at wavelengths between 10 and 100 μm is 70/109 (64%). Thus, it is possible to present a comprehensive picture of the far-infrared energy distribution of optically selected quasars, and, using these data and data at other wavelengths, to discuss the origin of the infrared continuum.

It is generally accepted that emission from heated dust produces the far-infrared continua of type 2 Seyfert galaxies and luminous *IRAS* galaxies. It is also generally acknowledged that the rapidly variable infrared emission in the BL Lacs and optically violently variable quasars must be produced by nonthermal processes. Thus thermal and nonthermal emission evidently occurs in objects of comparable luminosities. Both are probably present at a nonnegligible level in all quasars. In this paper, we address the possibility of thermal emission, which we believe produces the dominant emission in most quasars. Many authors have previously suggested that there might be thermal dust contributions to various portions of the infrared spectra of quasars—particularly to the so-called "3 μm bump" and near-infrared excesses (e.g., Rees *et al.* 1969; Bollea and Cavaliere 1976; Hyland, Becklin, and Neugebauer 1978; Neugebauer *et al.* 1979; Rieke and Lebofsky 1981; Hyland and Allen 1982; Carleton *et al.* 1987; Ward *et al.* 1987; Edelson and Malkan 1986; Barvainis 1987; McAlary and Rieke 1988; Chini, Kreysa, and Biermann 1988; Clavel, Wamstecker, and Glass 1989). We argue that almost *all* features of quasar continuum spectra, with the exception of the X-ray emission, can be understood as emission from a central accretion disk, reprocessed by a more-or-less continuous warped disk of material extending from the accretion disk to the outskirts of the host galaxy. The warped disk geometry, suggested

[1] Presidential Young Investigator.

by the morphology of the ISM in nearby normal and Seyfert galaxies, naturally avoids problems of self-shielding and reddening which had been raised as objections to earlier models.

To simplify the reader's task, we have removed many details from the body of the text. The sample of PG quasars is defined in § II, and the continuum energy distributions are presented in § III. Section IV explains why we think thermal emission is a significant, and probably dominant, cause of the infrared emission in most quasars. Section V discusses nonthermal contributions to quasar continua. Section VI outlines observational tests that can be used to determine whether thermal or nonthermal emission dominates in the submillimeter and infrared. A new infrared luminosity function is presented in § VII, and its significance for the covering factors of quasars is discussed, Section VIII summarizes the major results. The details of the data are given in Appendix A, and possible observational tests to discriminate between thermal and nonthermal mechanisms in the infrared and submillimeter are presented in Appendix B. The details of §§ IV and V can be found in a companion paper (Phinney 1989*b*). A reader wanting a quick overview of our paper should look at Figures 1, 3, 7, 8, and read § VIII.

II. THE SAMPLE

The sample of 109 objects discussed in this paper includes the 105 PG bright quasars listed in Neugebauer *et al.* (1987) plus four additional PG bright quasars, PG 0050+124 (I Zw 1), PG 1322+659, PG 1425+267 (Ton 202), and PG 2214+139 (Mrk 304). For historical reasons, as described in Neugebauer *et al.* (1987), the current list of PG bright quasars differs slightly from the final source list of 114 objects published by Schmidt and Green (1983).

III. THE RADIO TO X-RAY CONTINUUM ENERGY DISTRIBUTIONS

Most of the observations of PG quasars come from several recently published surveys. Neugebauer *et al.* (1987) have presented nearly simultaneous observations from 0.3 to 2.2 μm of 105 of the PG quasars, and a 6 cm survey of 102 PG quasars has recently been obtained by Kellerman *et al.* (1989). X-ray data for $\sim$60% of the PG quasars are given in Tananbaum *et al.* (1986), and observations at millimeter wavelengths have been reported for $\sim$30 PG quasars (Chini, Kreysa, and Biermann 1988; Keene *et al.* 1988). New flux densities reported in this paper are from the *IRAS* survey and from new observations with the Palomar 5 m telescope. These data, along with previously published data for PG quasars, are described in detail in Appendix A.

Figure 1 presents the continuum energy distributions for the PG quasars. The continuum distributions are well determined throughout the wavelength range 0.3–2.2 μm from the data of Neugebauer *et al.* (1987). The available far-infrared data are sufficient to allow a good determination of the shape of the continuum out to $\sim$100 μm for nearly two-thirds of the sample. Low *et al.* (1989) have also analyzed *IRAS* data for PG quasars in the context of comparing these quasars with infrared selected quasars. In general, the infrared properties of the PG quasars reported by Low *et al.* are consistent with what is reported here. Figure 1*a* shows the shape of the continuum energy distributions in the quasar rest frame for all 70 objects detected at more than one wavelength between 10 and 100 μm. A smooth curve has been drawn to represent the infrared-optical-UV continuum. "Radio-loud" and "radio-quiet" objects have been plotted in separate columns for purposes of display.

Figure 1*b* shows the energy distributions for the 39 objects not detected at any wavelength between 10 and 100 μm. As discussed in Appendix A, the main reason that this second group of sources was not detected in the infrared is that they were, in general, more distant. The upper limits of Figure 1*b* are consistent with the distribution of detections. The far-infrared properties of the PG quasars will be discussed using only the objects in Figure 1*a*; it seems reasonable to assume that the far-infrared properties of the nondetected sources are not different from those for the detected sources.

Figure 1 gives a clear picture of the energy distributions over eight decades in wavelength, $\sim$0.3 nm to 6 cm ($10^{9.7}$–10^{18} Hz), for the PG quasars. It is evident that emission at wavelengths 3 nm to 300 μm (10^{12}–10^{17} Hz) dominates the total energy output of all PG quasars regardless of the radio properties or the bolometric luminosity. A large fraction of PG quasars emit more than 20% of their bolometric luminosity at wavelengths between $\sim$1.5 and 100 μm, and there are a few objects (e.g., PG 0157+001, PG 0931+437, and PG 1543+489) that appear to emit more than half of their total bolometric luminosity at these wavelengths. In addition, the general shapes of the energy distributions of all PG quasars are remarkably similar. The infrared-optical-UV continuum dominates the energy output in every case. Beyond 100 μm the energy emitted falls rapidly, and a more modest decrease is observed at soft X-ray wavelengths. The largest variation appears to be at radio wavelengths where the difference in radio power relative to the infrared maximum between radio-loud and radio-quiet quasars is a factor of $\sim 10^3$.

a) Mean Energy Distributions

Figure 2 presents average continuum energy distributions of the PG quasars detected between 10 and 100 μm. The distribution are normalized at 1 μm. All of the PG quasars appear to emit the bulk of their luminosity (typically more than 90%) in the wavelength range $\sim$30 nm to 300 μm (10^{12}–10^{17} Hz). Over this range of wavelengths, all quasars have remarkably similar spectral energy distributions. This universal distribution can plausibly be fitted by two broad components, as illustrated in Figure 3 where three examples representing different radio power and radio spectral index are displayed. The two components can be described as an "infrared bump" that dominates the emission in the wavelength range $\sim$2–300 μm (10^{12}–$10^{14.2}$ Hz), and the "big blue bump" (Malkan and Sargent 1982) that dominates the emission at wavelengths $\sim$10 nm to 0.3 μm (10^{15}–$10^{16.5}$ Hz). While additional continuum features may be present in this spectral range (e.g., the "3000 Å bump"), they constitute only minor perturbations in luminosity to the two components.

Past observations (e.g., Neugebauer *et al.* 1979, 1987) have characterized the infrared flux emitted by quasars in terms of a power law with spectral index $\alpha \sim -1 (f_\nu \propto \nu^\alpha)$. While such a characterization is valid over $\sim$1 decade in frequency, it is clear that a global view of the quasars' continuum requires a more complex description the energy distribution.

b) Bolometric Luminosity

The availability of data over a wide range of wavelengths allows a good determination of quasar bolometric luminosities. The bolometric luminosity, $L_{\rm bol}(H_0 = 75$ km s^{-1} Mpc$^{-1})$, was computed by integrating the flux densities over

(This Page Intentionally Left Blank)

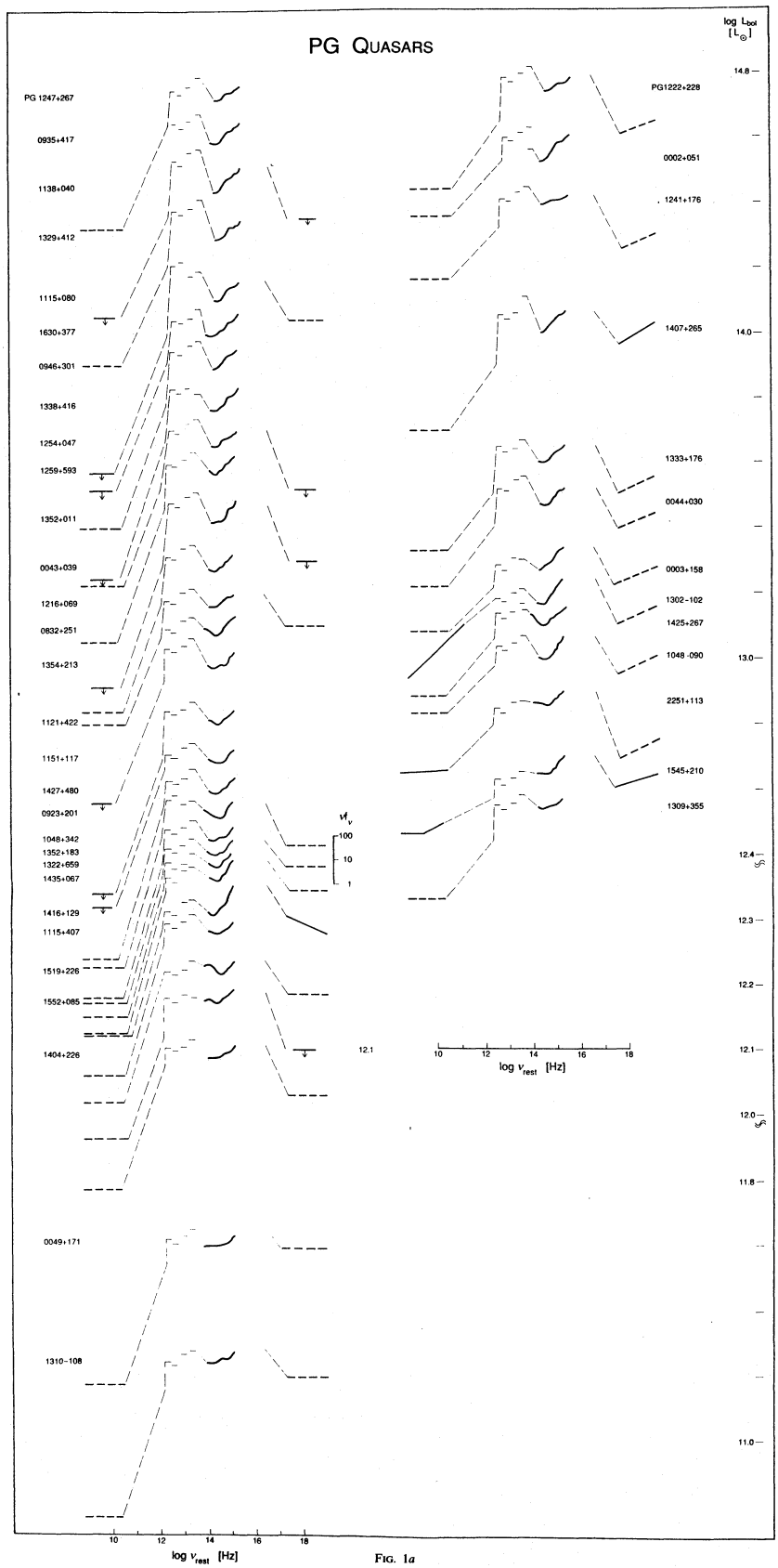

FIG. 1a

FIG. 1.—(*a*) Energy distributions from ~0.3 nm to 6 cm ($10^{9.7}$–10^{18} Hz) plotted as log νf_ν vs. log ν in the quasar rest frame, for PG quasars detected at wavelengths between 10 and 100 μm. Radio-quiet and radio-loud quasars are grouped on the left and right, respectively. The vertical scale corresponds to bolometric luminosity for the quasar in units of solar luminosity for assumed Hubble constant $H_0 = 75$ km s^{-1} Mpc^{-1} and $q_0 = 0$. The distributions are plotted such that the value of νf_ν at log $\nu = 14.5$ corresponds to the bolometric luminosity. The source name is printed at that same vertical level. Thick solid lines represent a smooth fit to the observed data points. In the radio, where most objects have been observed only at 6 cm, a thick horizontal dashed line represents an assumed spectral index $\alpha = 1$ ($f_\nu \propto \nu^\alpha$) for both radio-quiet and steep-spectrum radio-loud quasars. At X-ray wavelengths, the thick dashed line through the 2 keV data point assumes a spectral index of 1 and 0 for radio-quiet and radio-loud objects, respectively. Thin dashed lines connect the observed far-infrared data to the extrapolated radio data. The shape of the "big blue bump" between wavelengths ~ 10 nm to 0.1 μm ($10^{15.5}$–$10^{16.5}$ Hz) is unknown; a thin dashed line extrapolates the high-frequency edge of the bump at log $\nu = 16.5$ Hz (with an assumed height equal to the last observed UV data point near log $\nu = 15.5$ Hz) to the X-ray data. (*b*) Energy distributions for PG quasars not detected at wavelengths between 10 and 100 μm. Individual curves are drawn as described in (*a*) except that only upper limits are shown for the wavelength region 10–100 μm.

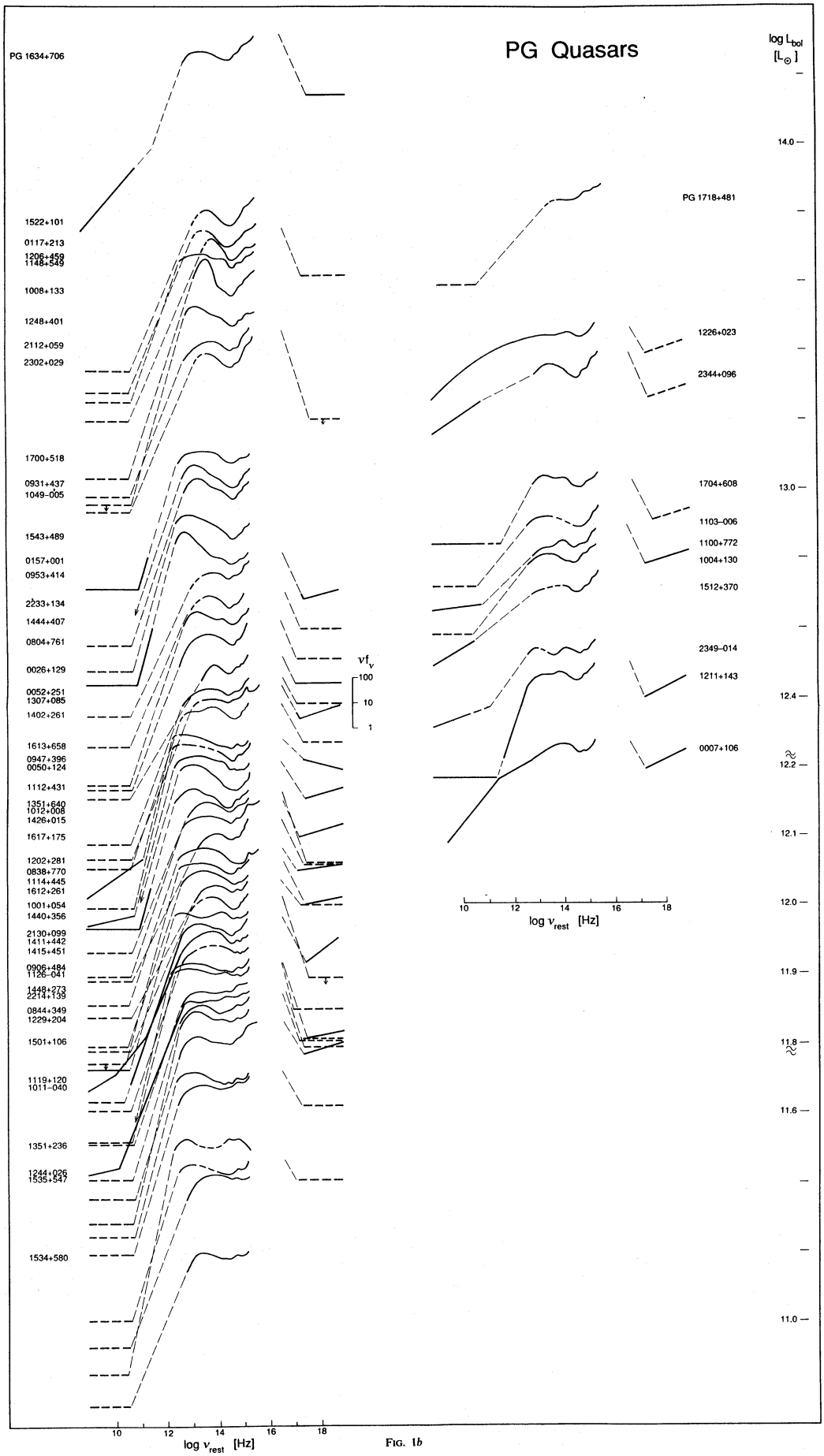

FIG. 1*b*

(This Page Intentionally Left Blank)

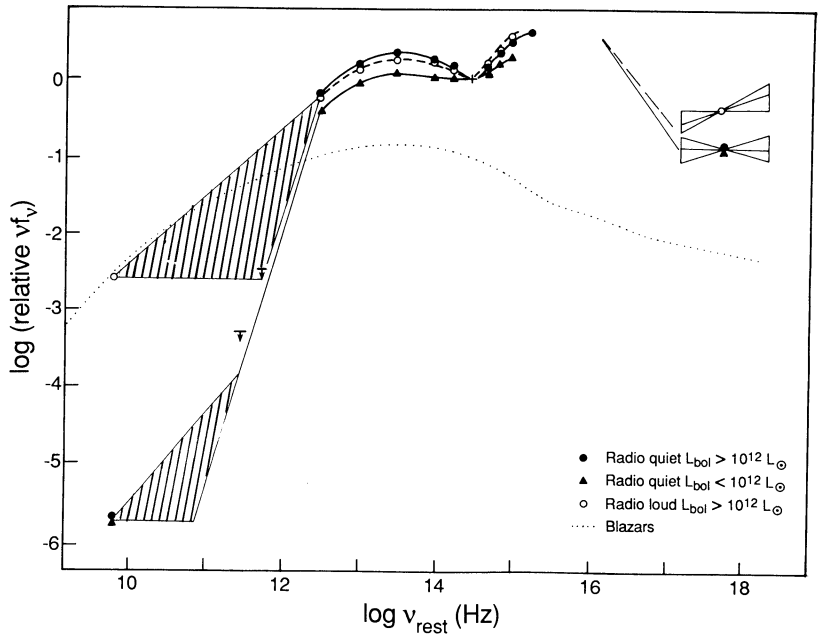

FIG. 2.—Average continuum energy distributions for radio-loud and radio-quiet PG quasars. The data points are mean values for the quasars in Fig.1. Variations in the mean are typically 0.15 in the log for the far infrared data, and 0.1 in the log for the near-infrared and optical data. The X-ray slopes are adopted from Wilkes and Elvis (1987). The hatched region at radio-submillimeter wavelengths represents the range of spectral indices observed. Shown for comparison (*dotted line*) is the mean continuum energy distribution for blazars (Impey and Neugebauer 1988), normalized at 6 cm (see text).

the frequency range 10^{12}–10^{17} Hz for those quasars with reasonably well determined far-infrared spectra (i.e., Fig. 1*a*). This procedure is sufficient to provide an accurate measure of the true bolometric luminosity since emission at higher and lower frequencies appears never to account for more than 5% of the total. For the "big blue bump," the shape was assumed to be that shown by the solid line in Figure 1*a* with the additional assumption of a flat region, constant in νf_ν, to bridge the gap from $10^{15.3}$ to $10^{16.5}$ Hz; ν is the frequency and f_ν is the flux density. This approximation is equivalent to increasing the integrated emission in the observed portion of the continuum between $10^{14.5}$ and $10^{15.3}$ Hz by a factor of 7 to approximate the luminosity in the range $10^{14.5}$–10^{17} Hz. Figure 4*a* shows that the bolometric luminosities of the PG quasars in Figure 1*a* vary over nearly a factor 10^3. Figure 4*b* shows the ratio $L_{bol}/\nu L_\nu(B)$ for the same sample of PG quasars in Figure 1*a*; $L_\nu(B)$ is the luminosity density at a wavelength of 0.4 μm. The range of a factor ~ 2 in this ratio illustrates mainly the range of the relative contribution of the infrared emission. The mean value of $L_{bol}/\nu L_\nu(B)$ is 16.5.

The energy distributions in Figure 1*a* have been used to test whether bolometric luminosity is an important parameter in determining the relative strengths of the infrared and blue bumps. Figure 5*a* shows that the strength of the infrared bump, as measured by the height of the peak of the infrared bump above the 1 μm dip, is independent of L_{bol} for $L_{bol} > 10^{12}\ L_\odot$. There is perhaps a decrease in the strength of the infrared bump for $L_{bol} < 10^{12}\ L_\odot$. Figure 5*b*, comparing the relative strengths of the infrared and blue bumps, also shows no obvious dependence on L_{bol}, except possibly for a systematic smaller ratio at $L_{bol} < 10^{12}\ L_\odot$. The mean ratio of bump luminosities, L_{IR}/L_{UV}, is 0.4 ± 0.15.

Figure 2 emphasizes the results of Figure 5 by showing that the mean energy distribution for quasars with $L_{bol} < 10^{12}\ L_\odot$ is flatter than the mean energy distribution of the more luminous quasars. The "flattening" of the energy distribution at $L_{bol} < 10^{12}\ L_\odot$ is similar to the result found by Kriss (1988) for radio-quiet quasars. This flattening in the lowest luminosity quasars could well be due to the contribution in the near-infrared and optical of starlight from the host galaxy. Neugebauer *et al.* (1985) have shown that at 1.3 μm the extended emission around the lowest luminosity quasars has luminosity comparable to that of the unresolved source.

c) *Radio Loud versus Radio Quiet*

Figure 6*a* shows the distribution of ratios of radio to 1 μm brightness for 102 PG quasars in the 6 cm survey of Kellerman *et al.* (1988). Including the few upper limits, the ratio of radio to 1 μm luminosity has a range of more than 10^5. There is a clear concentration of "radio-quiet" sources near the ratio $\log [\nu f_\nu (1\ \mu\text{m})] = -5.5$ and a smaller, less well defined grouping of "radio-loud" objects with a ratio near -2.5. Both peaks are broad enough to make the distinction between radio-loud and radio-quiet ambiguous in $\sim 10\%$ of the PG quasars. For the current discussion the separation is arbitrarily made at the value $\log [\nu f_\nu (6\ \text{cm})/\nu f_\nu (1\ \mu\text{m})] = -4$.

The large differences in radio properties appear, for the most part, to be decoupled from emission at wavelengths less than ~ 1 mm. Figure 2 shows the range of shapes of the radio continuum energy distributions for radio-loud quasars; their continua in the infrared and ultraviolet are indistinguishable from those of the radio-quiet quasars (see, e.g., Neugebauer *et al.* 1984, 1986). Although the radio data are sparse for radio quiet quasars, recent measurements at 21 cm and 2 cm (Antonucci and Barvainis 1988*b*) for eight radio-quiet quasars show that the radio spectral index, α ($f_\nu \propto \nu^\alpha$), can vary between 0 and -1 as it does for radio-loud quasars. However, it is not yet clear whether the mechanism responsible for the range in spectral idex is similar for radio-loud and radio-quiet

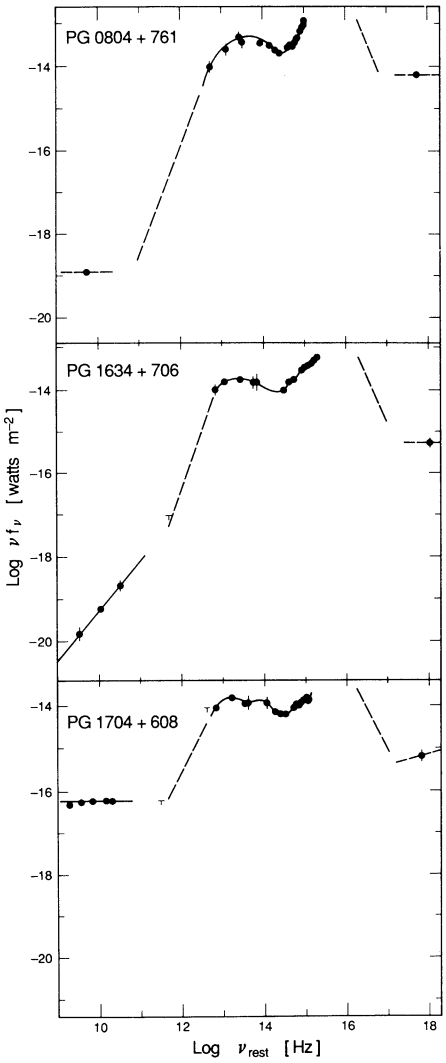

FIG. 3.—Examples of quasar energy distributions: (*top*) steep spectrum radio quasar, (*middle*) flat spectrum radio-quiet quasar, (*bottom*) steep spectrum radio-loud quasar.

quasars. For both the steep spectrum radio-loud quasars and all of the radio-quiet quasars, extrapolation of the radio continuum to shorter wavelengths misses the 100 μm point by factors of 10^2–10^6. Only in the case of the flat spectrum radio loud objects is there any indication that the radio emission may be directly coupled to the far-infrared data point at 100 μm.

At X-ray wavelengths there appears to be a small, but significant, difference between radio-loud and radio-quiet quasars (Wilkes and Elvis 1987). From Figure 2, radio-loud quasars appear, on average, to be twice as luminous at energies near 2 keV. The mean X-ray spectral index also appears to change from $\alpha = 0$ to $\alpha = -1$ for radio-loud and radio-quiet quasars, respectively. The X-ray spectral index would appear to imply a break near 0.1 keV, [log (ν/Hz) = 16.4], in the energy distributions of the majority of PG quasars if the high-frequency edge of the optical-UV bump falls as shown in Figure 2. For radio-loud quasars, the strength of the X-ray emission near 2 keV is typically a factor 5 less than the peak far-infrared emission; for radio-quiet quasars the 2 keV emission is typically a factor of 10 less than the far-infrared peak. For radio-loud quasars, the

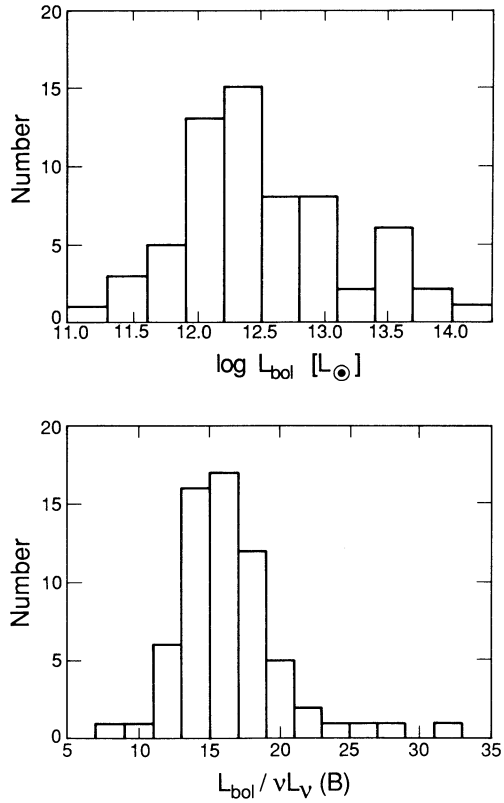

FIG. 4.—(*a*) The bolometric luminosity from 30 nm to 300 μm of PG quasars. (*b*) The ratio of bolometric luminosity to blue luminosity, νf_ν (0.44 μm).

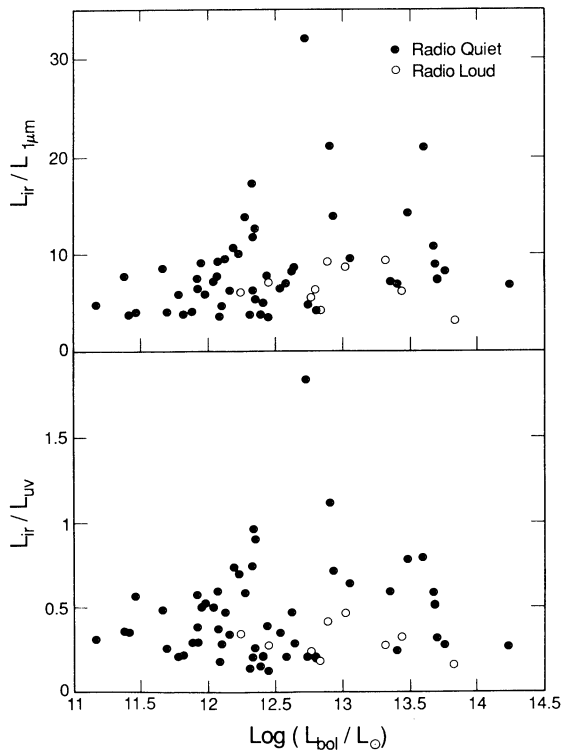

FIG. 5.—(*a*) The ratio, $R \equiv \nu f_\nu(6\text{ cm})/\nu f_\nu(1\ \mu\text{m})$, for PG quasars. Also shown for comparison is the ratio for blazars with $L_{bol} > 10^{12}\ L_\odot$, determined using data from Impey and Neugebauer (1988). (*b*) Same as (*a*) except for $R \equiv \nu f_\nu(6\text{ cm})/\nu f_\nu(\text{IR peak})$.

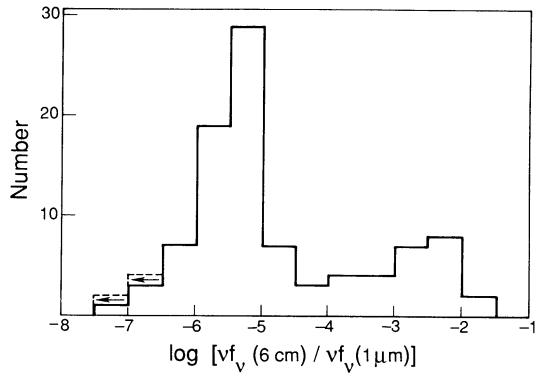

FIG. 6a

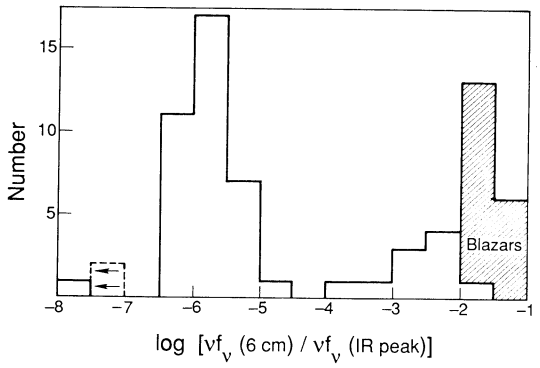

FIG. 6b

FIG. 6.—(*a*) Infrared "excess," $\log_{10} \int_{12}^{14.5} \nu f_\nu \, d \log \nu / \nu f_\nu(\log \nu = 14.5)$, as a function of bolometric luminosity. *Filled circle* (●), radio quiet; *open circle* (○) radio loud. (*b*) Ratio of "infrared bump," $\log_{10} \int_{12}^{14.5} \nu f_\nu \, d \log \nu$, to "blue bump," $\log_{10} \int_{14.5}^{16.5} \nu f_\nu \, d \log \nu \equiv 7 \times \log_{10} \int_{14.5}^{15.2} \nu f_\nu \, d \log \nu$, as a function of bolometric luminosity.

range of relative X-ray fluxes is approximately a factor of 5, while for radio-quiet objects the X-ray flux can vary by at least a factor 10 with a few objects having ratios $\nu f_\nu(25\ \mu\text{m})/\nu f_\nu(2\ \text{keV})$ greater than 400.

d) Relation to Blazars

Figure 6*b* shows the distribution of the ratio of the radio brightness to the infrared peak for 49 PG quasars and for 18 blazars as published by Impey and Neugebauer (1988). Although the radio-quiet and radio-loud peaks are better separated than in Figure 6*a*, the ratio of the radio brightness to the 1 μm flux density (Fig. 6*a*) was used in the definition of the radio types since it was available for all the PG quasars.

In terms of the degree of radio loudness, the radio-loud PG quasars bear the closest resemblance to blazars. Blazars, however typically do not show a strong optical-UV bump, and, as shown in Figure 6*b*, their radio properties are more extreme than those of the radio-loud PG quasars. If the radio-loud quasars contain jets with radio to infrared continua similar to those of blazars, Figure 2 shows that they would not contribute significantly to the infrared fluxes of all but the most "blazar-like" of the radio loud PG quasars, (e.g., 3C 273 = PG 1226+023).

IV. THERMAL CONTRIBUTIONS TO THE QUASAR INFRARED CONTINUUM

a) Overview

We implicitly assume the ultimate source of the luminosity in quasars is the release of gravitational energy by matter in an accretion disk falling into a black hole. Furthermore, the emission in both observed bumps shown in Figures 1–3 is attributed to thermal radiation. We, along with others (e.g., Shields 1978; Malkan and Sargent 1982; Czerny and Elvis 1987), assign the "big blue bump" in the ultraviolet to partially thermalized emission from gas at temperatures 10,000 to 100,000 K in the accretion disk of quasars. Figure 7 presents a schematic view of the model that will be discussed for the production of the infrared radiation. We will show that the infrared flux at wavelengths from 1 to 300 μm in most PG quasars can be accounted for by reradiation of the central luminosity by gas and dust in warped disks in the host galaxies of the quasars.

The 0.5–5 μm radiation in quasars can be attributed to reradiation from heated gas and dust in the outer edge of the accretion disk and in a disk of molecular gas within a few parsecs of the central energy source. The disk is shielded from direct radiation from the central source, but radiation will be scattered into the disk by the clouds of the broad-line region and any intercloud medium. The reradiation from this heated gas and dust must contribute a significant, and plausibly dominant, fraction of most quasars' near-infrared luminosity.

A striking feature of Figure 1*a* is the universality of the local minimum in νf_ν at $\nu = 10^{14.5}$ Hz, ($\lambda = 1\ \mu$m), previously noted by Neugebauer *et al.* 1987. The frequency of this minimum is the same in objects differing in bolometric luminosity by 10^3 and in radio luminosity by 10^5. Such constancy suggests that the frequency of the minimum is related to some fundamental physical or atomic constants rather than to an accident of absorption or to the superposition of environment-dependent radiation processes. We show that the dip is plausibly due to a drop in opacity caused by the sublimation of the most refractory grains at temperatures $T \sim 2000$ K and the consequent heating of the gas, which is optically thick to the incident radiation, to temperatures $T \gtrsim 10{,}000$ K. Thus we argue that the emission near 1 μm is due to optically thin free-free radiation from the externally heated gas of the outer accretion disk.

We attribute the radiation from 5 to 1000 μm to energy reradiated by dust in warped disks at distances beyond several parsecs. The warps and scale heights of nearby normal galaxies are such (Genzel and Townes 1987; Bosma 1983) that if they contained a quasar, *at least* 10% of a central quasar's luminosity would be absorbed and reradiated in the infrared. It seems inescapable that a large fraction of all quasars' far-infrared luminosity is due to reradiation from their disks. Gas and dust in the quasars' host galaxies are almost certainly exposed to the radiation from the inner regions of the accretion disk, as well as to any reradiation from gas and dust at smaller radii. Gravitational instabilities make it unlikely that the $\sim 10^8$ $M_\odot$ accreted by the central black hole during the lifetime of a quasar, $\sim 10^8$ yr (Phinney 1989*b*), can be stored at radii less than a few parsecs. Thus the reservoir of gas must extend *at least* to several tens of parsecs. Such gas has been identified in many galaxies; it rarely occupies a single plane, and would therefore be directly exposed to radiation from the central accretion disk. A tilted disk of gas extending beyond 2 pc from the center has been seen in the Galaxy (Genzel and Townes 1987), and similar, but even more severely tilted disks have been identified in many Seyfert galaxies (Unger *et al.* 1987; Krolik and Begelman 1988).

Our picture differs from previous work in placing the dust and gas in a disk rather than in isotropically distributed clouds such as the broad-line clouds (Rees *et al.* 1969; Bollea and Cavaliere 1976; Puetter and Hubbard 1985; Barvainis 1987; the latter also considers conically symmetric distributions). We

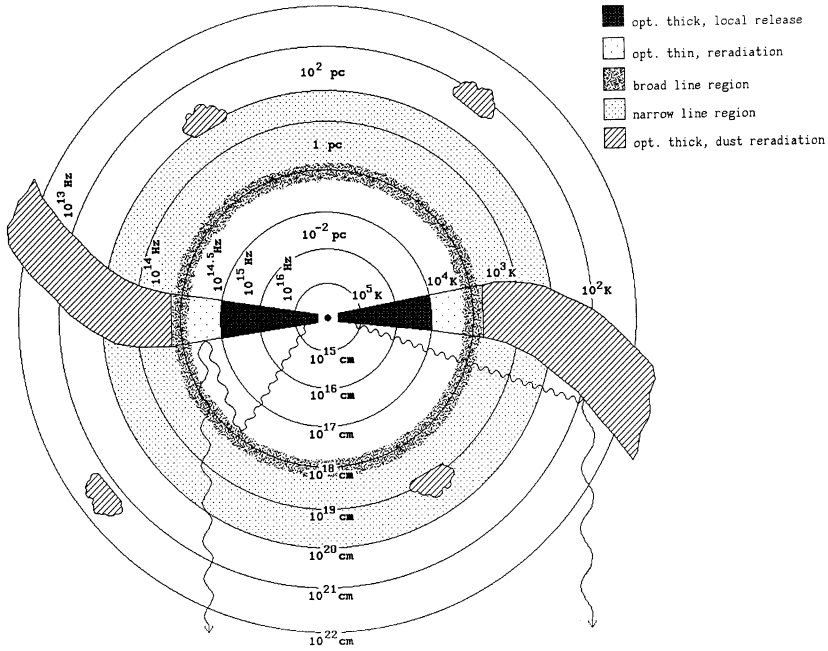

FIG. 7.—Cartoon illustrating our model for the 10^{12} to 10^{16} Hz emission for radio-quiet quasars. Only thermal emission processes are involved. Continuum emission at frequencies above $10^{14.7}$ Hz comes from $r < 10^{17}$ cm where the energy source is local release of gravitational binding energy. Emission at lower frequencies is reradiation from a gas disk (and perhaps some high latitude clouds). Free-free emission from gas whose dust has sublimated ($10^{17} < r < 10^{18}$ cm) contributes in the near infrared. Reradiation from dust at radii $> 10^{18}$ cm dominates at frequencies below $\sim 10^{14.2}$ Hz.

believe that our picture is more probable on physical grounds, not least because the molecular gas and dust in galaxies is observed to be in lumpy disks, not in spherically symmetric distributions of clouds. Dust in a disk has several other desirable properties. First, the lifetime of dust in a partially shielded thicker disk can be higher than that of dust in clumps within the broad-line region of quasars which would have only a very short lifetime against sputtering. Second, clouds in a disk illuminated from above will survive longer than dusty clouds which are directly exposed to the central radiation source and, within ~ 100 pc of the central source, would be driven outward by radiation pressure. Third, the gas in the disk has a column density high enough to produce the observed 1 μm radiation by free-free emission, whereas standard broad-line clouds probably do not (Puetter and Hubbard 1985). Fourth, a warped disk model offers the attractive feature that the inner regions do not necessarily obscure the outer regions. In this picture, dust at distances $r \gtrsim 100$ pc from the central source is directly illuminated by short-wavelength radiation from the central source. Thus substantially lower masses of dust are required than if the outer regions were shielded by the dust in the inner regions (as considered by Barvainis 1987, his eq [11]), and were primarily iluminated by longer wavelength reradiation from dust at $r \lesssim 100$ pc, which they absorb only inefficiently.

b) Model

In what follows, we discuss a model for a typical quasar. In reality the detailed structure of the disk is more complicated than we assume. The disk is locally self-gravitating, is likely to be clumpy and may form stars. These complications are irrelevant to the present discussion, provided the covering factor remains large along the line of sight to the central course. Detailed calculations of the emergent energy from the assumed model, which result in Figure 8, are given in Phinney (1989*b*, *c*).

The shape of the infrared continuum depends on the distribution of dust mass as a function of temperature. In our model this distribution depends on the warp angles, and to a lesser extent, the amounts of gas in the galaxy. Quasars with small warps and thin disks have weak far-infrared emission. Quasars with warps which are larger at large radii (and hence slightly larger minimum dust masses at large radii) have steeper infrared continua. The range of continuum shapes shown in Figure 1 is not surprising, since a great variety of gas structures is to be expected in the disturbed host galaxies. Figure 1 should also be compared with Figure 15 of Sanders *et al.* 1988*a*, which includes objects of similar luminosities but without ultraviolet excesses.

The temperature of dust at a distance r and extinction optical depth τ from a central source of luminosity L_c has temperature T_d given implicitly by

$$\sigma T_d^4 \langle Q_e(a, T_d)\rangle = \frac{L_c e^{-\tau}}{16\pi r^2} \langle Q_a\rangle . \quad (1)$$

Here σ is the Stefan-Boltzmann constant, $\langle Q_a\rangle$ is the absorption efficiency (absorption cross section over the geometric cross section) averaged over the incident spectrum and the size distribution of dust grains, and $\langle Q_e(a, T_d)\rangle$ is the *emission* efficiency averaged over the emergent rest wavelengths for a Planck spectrum with temperature T_d, $\langle Q_e(a, T_d)\rangle = (\pi/\sigma T_d^4) \int_0^\infty Q_a(a, \nu) B_\nu(T_d) d\nu$; $B_\nu(T_d)$ is the Planck blackbody function per unit solid angle (see, e.g., Draine and Lee 1984). Typically $\langle Q_e(a, T_d)\rangle \propto a T_d$ and $\langle Q_a\rangle$ depends on the size a of the grains and on the spectrum of incident radiation, but is independent of T_d. Fits for these parameters have been taken from Draine (1981) and Jura (1982). The distribution of grain sizes a was assumed to be the MRN distribution (Mathis, Rumpl, and

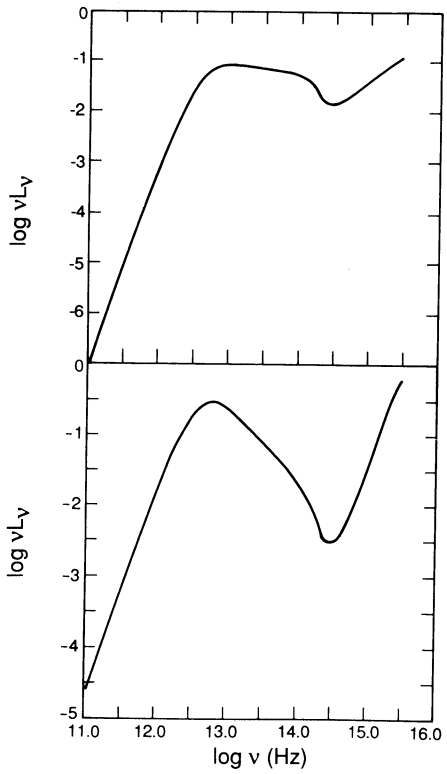

FIG. 8.—(*a*) Spectrum produced by a disk whose warp angle (at radii $r > 10^{18}$ cm) increases linearly with log r. The minimum dust temperature was taken to be 50 K, and the dust absorption efficiency to scale as $Q_a \propto \nu^1$. Thus the flux low frequencies scales as $F_\nu \propto \nu^3$. The broad-line region (at $r = 10^{18}$ cm) was assumed to scatter 10% of the radiation generated by the accretion disk at smaller radii, where a Newtonian α disk with $\alpha = 0.1$ and $L = 0.5L_{\rm Edd}$ for $M = 10^8\ M_\odot$ was assumed. The flux from the disk is plotted only to $10^{15.5}$ Hz, beyond which relativistic effects and the detailed inner structure of the disk become important. (*b*) As in (*a*), except the warp angle of the outer disk increases as $(\log r)^2$, and very large dust grains ($a > 10$ μm) were assumed, so Q_a = const. The latter affects only the slope of the submillimeter spectrum, which here scales as $F_\nu \propto \nu^2$.

Nordsieck 1977). The resulting median dust temperatures, T_d, as a function of distance from the central source, are given in Table 1, along with the minimum masses of dust required to produce the emission within each decade in radius. This minimum mass of dust is defined by setting the absorption optical depth along the line of sight to the central source to unity. For definiteness in computing the values in the table, a hypothetical "typical" quasar with infrared spectral index from $10^{12.5}$ to $10^{14.5}$ Hz of -1, a bolometric luminosity of $10^{12.4}\ L_\odot$, and a total infrared luminosity of half of the UV luminosity was considered.

TABLE 1

DUST EQUILIBRIUM TEMPERATURES AND MASSES[a]

r (pc)	10^{-1}	1	10	10^2	10^3	10^4
T_d (K)[b]	3500	1250	450	160	60	20
Peak wavelength (μm)	...[c]	3	8	25	60	180
$M_{\rm dust}(<r)\ (M_\odot)$[d]	...[c]	0.2	20	$10^{3.3}$	$10^{5.3}$	$10^{7.3}$

[a] For a quasar with $\log(L_{\rm bol}/L_\odot) = 12.4$ or $L_{\rm bol} = 10^{46}$ ergs s^{-1}.

[b] Median dust temperature at distance r, for standard MRN distribution of grain size (Mathis *et al.* 1977). If all grains at r are larger than ~ 1 μm, the temperature will be ~ 2 times lower. If all grains at r are smaller than ~ 0.1 μm, the temperature will be ~ 2 times higher.

[c] Dust at this temperature would have sublimated.

[d] Minimum required mass of dust *interior* to radius r. If all grains within r are smaller than ~ 0.1 μm, the dust mass will be ~ 5 times lower. If all grains within r are larger than ~ 1 μm, or are not directly exposed to UV radiation, the required dust mass is ~ 10 times higher.

i) *Role of the Accretion Disk*

The ultimate source of energy for the infrared radiation must be within a few gravitational radii of the black hole ($\sim 10^{-4}$ pc) since the energy liberated per octave in radius in an accretion disk scales as r^{-1} (Shakura and Sunyaev 1973; Novikov and Thorne 1973). If the infrared radiation were emitted from a region comparable in size to that of its energy source, the brightness temperature would be so high that a nonthermal emission mechanism would be required. If the emission is thermal, the temperature of the region contributing radiation at wavelength λ cannot much exceed $hc/(4k\lambda)$, or it would produce too much flux at shorter wavelengths. The blackbody limits on the source size at 1 μm and at 60 μm are, respectively, more than 0.5 pc and more than 1000 pc for the most luminous sources in Figure 1*a* and more than 0.01 pc and more than 20 pc for the least luminous. Hence thermal infrared emission must be emitted at radii so large that local release of gravitational energy cannot be important. The flux must be reprocessed energy transported from the much smaller region of generation to the emission radii. The transport may be by radiation or by mechanical means (e.g., a jet or wind). For simplicity, we consider only the former, which seems to be adequate.

ii) *The Transition Disk: Near-infrared*

We interpret the 0.5–5 μm continuum as thermal emission from the outer accretion disk (0.1–1 pc) heated by radiation from the broad-line clouds. The emission from 2 to 5 μm we interpret as reradiation from heated dust grains, while the emission between 0.5 and 2 μm we interpret as free-free emission from gas at smaller radii, heated to more than 10,000 K after its dust has been sublimated.

The accretion disk will intercept between one-third and one-half of the reradiation from the broad-line region (BLR) clouds depending on whether the clouds are close to the disk or are spherically distributed. Photoionization models predict that the radius of the BLR is $\sim 0.3(L_{\rm UV}/10^{12}\ L_\odot)^{1/2}$ pc (e.g., Krolik, McKee, and Tarter 1981), comparable to the radius of a dust disk emitting the observed luminosities at 2–5 μm. The covering factor of the BLR clouds at radii ~ 0.1–1 pc can be estimated from line equivalent widths and X-ray absorption to be $\Omega/4\pi \sim 0.1$ for quasars (e.g., Ferland and Shields 1985). Since the intercloud medium may have an optical depth to electron scattering greater than 0.1 (Kallman and Krolik 1986), a minimum of 0.05–0.2 of the quasar's UV luminosity will be reprocessed into infrared radiation by the disk (see also Collin-Souffrin 1987). In any case, this reprocessed fraction is comparable to the fraction actually observed in 0.5–5 μm emission in the objects of this sample.

In the region of the disk within the inner few parsec, the gas and dust temperatures are closely coupled, and at temperatures $T_d < 2000$ K the opacity of the disk is largely due to dust. In fact, the required amounts of dust can persist and grow in the dense outer accretion disk to provide the emission observed in the 2–5 μm continuum. About 1 $M_\odot$ of dust is required in the inner parsecs (see Table 1). Red giant stellar winds in the inner parsec supply at most $\sim 10^{-5}\ M_\odot$ yr^{-1} in dust (thus requiring a dust lifetime $\sim 10^5$ yr if they were the

sole source), while dust cannot be transported from larger radii in less than the crossing time ~ 1 pc per 1000 km s^{-1} $\sim 10^3$ yr. Dust is destroyed by sublimation, but can also grow by accretion of gas-phase carbon. If grain growth is temporarily neglected, the above considerations show that the lifetime of any grains numerous enough to make the disk optically thick must be at least 10^3 yr, so if the grains are 0.1 μm in radius, their sublimation rate must be less than 0.1 μm/10^3 yr, hence, as shown by Phinney (1989*b*), the temperature *in vacuum* would have to be less than 1600 K.

The density and temperature conditions in this portion of the disk are quite similar to those in the ejecta of late-type stars, so grains can continue net growth to $T = 2000$ K if there is sufficient gas phase carbon (Phinney 1989*b*). A further temperature increase as small as ~ 100 K will cause the grains to sublimate on time scales shorter than 1 day, and a mechanism must be found to cool the gas. Other processes tending to destroy grains, such as sputtering, grain-grain collisions in shocks, surface reactions with other elements (e.g., oxygen), and damage by high-energy particles can only reduce the maximum temperature. Thus 2000 K is a stringent upper limit to the grain temperature. Even with a maximum temperature of 2000 K, the flux from dust in the disk will have dropped below an extrapolated power law by a factor of 2 at $10^{14.3}$ Hz, and by a factor of 10 at $10^{14.5}$ Hz. The inner portions of the accretion disk, powered by local release of gravitational energy, do not contribute significant flux at these long wavelengths. The shallow minimum at ~ 1 μm cannot, therefore, be explained solely by dust sublimation plus a contribution from an optically thick accretion disk.

We believe that the emission at ~ 0.5–1 μm is likely to be optically thin emission from the partially ionized disk interior to the point at ~ 0.1 pc where the dust is sublimated (Fig. 7). When the dust sublimates, the opacity, and therefore radiation efficiency of the disk suddenly drops. The disk would then be unable to stay in thermal equilibrium if it remained at the temperature of ~ 2000 K. Phinney (1989*b*) concludes that the disk finds a new stable equilibrium, cooled by optically thin free-free emission, at a temperature greater than $\sim 10{,}000$ K. The low opacity and cooling rate of gas in the intermediate temperature range $2000 < T < 10{,}000$ K means that it is thermally unstable, and therefore unlikely to be present in substantial quantity. As illustrated by Figure 8, the absence of gas at intermediate temperatures means that the reradiated continuum will have a minimum in νf_ν at $\nu \sim 10^{14.5}$ Hz, coincident with the observed minimum.

iii) *The Outer Disk: Far-infrared*

We now consider emission from disk material at distances greater ~ 10 pc, that contributes to emission at wavelengths of 5–1000 μm. As shown below, the gas and dust radiating at these wavelengths must be exposed directly to the nuclear emission. To avoid shadowing, the clouds must be at high latitudes with respect to the inner accretion disk. One simple way to arrange this is to have the disk warp. Although there is no direct evidence that this is the case for the PG quasars, warps seen to be very common in their low-luminosity cousins. The parsec-scale dust torus in NGC 1068 (Antonucci and Miller 1985) has its axis at right angles to the kiloparsec-scale disk of gas and stars (Wilson and Ulvestad 1982), and the axes of similar tori inferred to exist in other Seyfert galaxies make angles to the minor axes of the disks of their galaxies approximately uniformly distributed between 0° and 90° (Unger *et al.* 1987; Haniff, Wilson, and Ward 1988). Hence it seems likely that warps are common and substantial enough to allow the nuclear continuum to illuminate the dust and gas on scales of 10–1000 pc. It should be emphasized that infrared energy distributions alone cannot distinguish warped disks of gas from distributions of isolated clouds with the same covering factor as a function of radius. Galaxies are, however, observed to contain lumpy disks of gas, not isotropically distributed clouds.

The far-infrared emission cannot be powered by radiation scattered from the intermediate zone and the narrow-line region (NLR), located between 1 and $\gtrsim 1000$ pc (Fig. 7). The covering factor of the NLR clouds can be estimated by noting that cloud models give $L_{\rm NLR} \simeq 5 L_{[\rm O\ III]}$ (Ferland 1981). Shuder (1981) estimates that $L_{[\rm O\ III]} \simeq 0.02[\nu L_\nu(14.8)]$, so $L_{\rm NLR} \simeq 0.1[\nu L_\nu(14.8)]$, or $L_{\rm NLR} \simeq 0.006 L_{\rm UV}$ (Figs. 4 and 5). The covering factor of the NLR is thus $\Omega/4\pi \lesssim 0.01$. The luminosity between 5 and 1000 μm in most objects in the PG sample is thus too high to be explained by a disk reradiating emission from clouds in the narrow-line region. If a disk is to reradiate in the far-infrared, it must be distorted.

The shape of the thermal contribution to the spectrum from 5 to 1000 μm will depend on the distribution of covering factor (in a disk, warp angle) with radius. To produce $f_\nu \propto \nu^{-1}$ requires an equal covering factor between every octave in radius. Steeper spectra require larger covering factors at large radii. It would be surprising if all quasars had the same distribution of covering factor with radius. The wide range of shapes of the far infrared continua of quasars are apparent in Figure 1*a* and in Figure 15 of Sanders *et al.* (1988*a*). We discuss in § VII the appearance of quasars viewed from directions in which the dust disk obscures the central source.

c) *Implications*

i) *Radio to Millimeter Continuum*

The emission at wavelengths between 100 μm and 1 cm and ($10^{10.5}$–$10^{12.5}$ Hz) rises steeply, with $f_\nu \propto \nu^{1-2}$; several sources the emission rises more steeply than $f_\nu \propto \nu^{2.5}$ (Engargiola *et al.* 1988, Chini, Kreysa, and Biermann 1988; Edelson *et al.* 1988). Such a steep rise requires the spectrum of the emissivity (or, in the optically thick case, the source function) to be even steeper. For optically thick dust, the source function is the Planck function, $\propto \nu^2$ at low frequencies. Host galaxies with reasonable masses of dust will, however, be optically thin at these long wavelengths. The absorption efficiency Q_a scales as ν^γ, with $0.6 < \gamma < 2$, depending on the grain shape and composition (Draine and Lee 1984; Wright 1987). The emissivity thus scales as $\nu^{2+\gamma} T_d$, where T_d is the dust temperature. A source with a well-defined minimum dust temperature would therefore have a steeply rising spectrum, as observed. The minimum temperatures inferred from fitting the energy distributions of Figure 1 range from 25 to 150 K. In order to preserve the steep spectrum, the luminosity of any components of dust with temperatures 0.3 and 0.1 of the inferred minimum temperature (making the dominant contribution at the point where νf_ν begins to roll over) must typically be less than 5% and 0.2%, respectively, of the luminosity of the dust at the minimum temperature. This does not require much contriving: Table 1 shows that dust exposed to the central source with temperature below the inferred minimum temperatures would lie at distances greater than a few kiloparsecs. The column density of molecular gas in normal galaxies falls rapidly beyond a few kpc

(see Young 1987), so the minimum temperature may be due to an absence of dust at large distances. Even if dust is present farther out, starlight keeps dust throughout galaxies heated to temperatures of the order of the inferred minima (e.g., Soifer *et al.* 1987; Rice *et al.* 1988), so dust far from, or shielded from the central nucleus will not necessarily be cooler. Starburst galaxies such as M82 and NGC 253 (whose submillimeter emission, is resolved and unambiguously thermal—Telesco and Harper 1980; Gear *et al.* 1986*a*, although it is a LINER with a weak nonthermal radio core: Norris *et al.* 1988) have spectra from 100 μm to 1 mm very similar ($f_\nu \propto \nu^{2.4-2.7}$) to those of the radio-quiet quasars in the PG sample and must have similarly well defined minimum temperatures.

ii) *Radio Emission*

We now inquire whether enough cosmic-ray electrons could be produced by stars, obviating the need for *any* nonthermal emission from the active nucleus, or whether the nucleus must produce the relativistic particles required to produce the radio emission of radio-quiet quasars. The radio luminosities are only one or two orders of magnitude brighter than the disks of normal bright spiral galaxies (Hummel 1981). Since the host galaxies of quasars are often accused of interaction and enhanced star formation (Hutchings 1983; MacKenty and Stockton 1984), the magnetic fields and cosmic-ray electron densities might well be higher than in normal spirals.

The ratio of far-infrared to 6 cm radio flux in the radio-quiet quasars (Fig. 6*b*) is, however, the same as that seen in normal and starburst galaxies: $\log \nu f_\nu|_{80\ \mu m} = 5.6 + \log \nu f_\nu|_{5\ GHz}$ (Fitt, Alexander, and Cox 1988; Helou, Soifer, and Rowan-Robinson 1985; De Jong *et al.* 1985; Gavazzi, Cocito, and Vettolani 1986). This surprising result has several possible interpretations. (1) Both the radio and far-infrared emission in radio-quiet quasars could be due to massive stars and their remnants. This seems unlikely, since the far-infrared spectrum in quasars joins smoothly to the near-infrared and optical, which is clearly not due to stars. (2) The radio emission could be due to electrons accelerated in supernova remnants, while the far-infrared emission could be reradiation from the nuclear source. This overcomes the objection to the first interpretation, but requires that the young stars in quasars be relatively more efficient at producing radio-emitting cosmic rays than stars in normal and starburst galaxies (perhaps because there is less dust to reradiate the starlight, or because the magnetic fields are higher than in normal and starburst galaxies). (3) The result could be entirely coincidental, neither the far-infrared emission nor the radio emission being related to stellar processes.

Conclusion 3 is supported by observations of the dust-shrouded active galactic nuclei Arp 220 and Mrk 231. Like the PG quasars, these have steeply rising submillimeter spectra, and a ratio of radio luminosity to $\nu f_\nu|_{80\ \mu}$ close to that for normal spiral galaxies. Yet most of the flux from Arp 220 comes from a radio core less than 60 pc in extent (Norris 1985), tiny compared with the infrared source ($\gtrsim$600 pc; Becklin and Wynn-Williams 1987) and the 18 kpc optical extent of the disk. Less than 5% of the total flux comes from a region more extended than 300 pc (Condon 1980). A point core in Mrk 231 contains 80% of the radio flux, while only 20% of the flux comes from an extended region comparable in size to the galaxy (de Bruyn and Wilson 1976). Although the radio emission might conceivably be due entirely to the host galaxy's disk, the ratio of far-infrared to radio emission requires some explaining. Weak radio jets or the nuclear accretion disk seem more plausible sources for the radio emission from the radio-quiet majority of quasars.

iii) *Stellar Contribution*

Dust heated locally by stars may contribute to some of the infrared emission from quasars. It is unlikely, however, that this dominates the continuum in the majority of sources. For stars to produce an infrared luminosity of $10^{13}\ L_\odot = 0.5\ M_\odot\ c^2\ yr^{-1}$ would require a star formation rate of *at least* 500 $M_\odot\ yr^{-1}$. This lower limit assumes that only massive O stars are formed; these process 20% of their mass from H to He, releasing 0.007 $M_\odot\ c^2$ per $M_\odot$. A normal interstellar mass function would require a rate $\sim$10 times higher. Over the $\sim 10^8$ yr lifetime of a quasar, greater than $5 \times 10^{10}\ M_\odot$ of gas would thus have to be processed in massive stars (see Phinney 1989*a* for details of this type of argument). Dust would form from the metals produced. So much gas and dust, pushed to high latitudes by supernova explosions, would inevitably absorb and reradiate much of the luminosity from the central source. But the optical and ultraviolet radiation from quasars, variable on time scales smaller than 10 yr (Usher 1978), must come from such a central relativistic source. Since its luminosity is comparable to the infrared luminosity, we conclude that reradiation from gas and dust heated by it would necessarily be *at least* comparable to anything contributed by stars.

V. NONTHERMAL CONTRIBUTIONS TO QUASAR CONTINUA

a) Overview

Arguments for a nonthermal origin for the far-infrared spectra of quasars have come primarily from studies of a very unrepresentative minority: the blazars and flat spectrum radio-loud quasars, which comprise only 5%–8% of the PG quasars (and indeed, of *all* optically selected quasars). In these sources, rapid variability (Roellig *et al.* 1986; Gear *et al.* 1986*b*; Edelson and Malkan 1987; Impey and Neugebauer 1988) and a few direct measurements (Backer *et al.* 1987, but see also Gear *et al.* 1985) require high brightness temperatures; much of their far-infrared emission is clearly nonthermal.

In core-dominated radio-loud quasars the near-infrared emission is most simply interpreted as optically thin synchrotron emission from the innermost parts of the jet, while the millimeter and radio emission comes largely from the synchrotron photosphere of the jet much farther out. (Blandford and Königl 1979; Reynolds and McKee 1980; Phinney 1983; Rees 1984; Blandford 1987). The slower variability at these longer wavelengths (Gear *et al.* 1986*b*; Impey and Neugebauer 1988) is consistent with this picture.

In the radio-quiet sources, a radio spectrum extrapolated as in the core-dominated sources would account for less than 0.1% of the far-infrared emission (Fig. 2). Nevertheless it has often been argued, by analogy with the core-dominated, radio-loud sources, that the infrared emission in all quasars is nonthermal.

3C 273, the brightest and the most extreme radio loud of the PG quasars with $\log [\nu f_\nu(6\ cm)/\nu f_\nu(1\ \mu m)] = -1.8$, is a curious intermediate case. Although a superluminal core-dominated radio source, it differs from other such objects in that it is normally only slightly variable in the infrared and is normally very weakly ($<$0.5%) polarized in the optical and near-infrared. It does, however, have spectacular (50%) flares, with rise times less than 1 day (Robson *et al.* 1986; Courvoisier *et al.* 1988) and is clearly ($\pm$50%) variable on time scales of months at wavelengths of 10 μm (Rieke and Lebofsky 1979; Neuge-

bauer *et al.* 1989) and 1 mm (Robson *et al.* 1986; Courvoisier *et al.* 1988). These flaring components are clearly nonthermal and highly ($\gtrsim 3\%$) polarized. However, since these amplitudes of variability and the quiescent polarization are low compared to those seen in many optically violent variables, it may be that during quiescence much of the infrared and optical emission is thermal, while the nonthermal emission from the jet dominates only during the most extreme outbursts.

b) X-Rays and Their Possible Relation to the Infrared

The claim that the 3 μm emission and 2 keV X-ray flux are closely linked (Malkan 1984; Elvis *et al.* 1986) has been used to support the view that the dominant radiation of Seyfert 1 galaxies and quasars is nonthermal. Malkan (1984) found an apparent correlation between the infrared and X-ray luminosities with an approximately constant value for the ratio $L(3\ \mu\text{m})/L(2\ \text{keV})$ for sources spanning 5 decades in luminosity. It was asserted that the X-ray flux was much more tightly correlated with the infrared than with the ultraviolet flux, suggesting that the infrared and X-ray emission was produced by the same particles. Similar correlations in heterogeneous samples have been found by Carleton *et al.* (1987) who find that the 3–10 μm luminosities are tightly correlated with the X-ray luminosities, while the ultraviolet and far-infrared luminosities are not. The most plausible models of this type produce the infrared by synchrotron emission, and the X-ray by Compton scattering (Zdziarski 1986; Band 1987).

It is not clear that such models are necessary. Most of the correlation in luminosity-luminosity plots of flux limited samples is simply introduced by the redshift. McAlary and Rieke (1988) have reexamined the infrared and X-ray properties of Seyfert 1 galaxies and quasars using more recent data and more complete samples. They find no correlation between the 3 μm and 2 keV fluxes for Seyfert 1 galaxies, and only a weak correlation between the 3 μm and 2 keV fluxes for PG quasars. For the quasars, the X-ray flux varied more nearly as the square of the infrared flux (with large scatter) rather than linearly with the infrared flux, as suggested by the previous heterogeneous samples.

Using the current data for the complete sample of PG quasars we have also reinvestigated the relation between the X-ray and 3 μm fluxes. Figure 9*a* shows that there is no strong evidence for any relation between these fluxes. In Figure 9*b*, the entire far-infrared component (2–100 μm) is compared with the X-ray emission (2–10 keV) again showing a complete lack of correlation between these two components. We conclude that there is no reason to invoke a common mechanism to account for the X-ray to far-infrared continuum of quasars.

c) Steepness of the Submillimeter Continuum

The steepness of the submillimeter continuum of quasars is difficult, but not impossible, to reproduce by nonthermal emission. The sources in which the flux density f_ν rises more steeply in the submillimeter than $f_\nu \propto \nu^{2.5}$ (see § IV*c*[i]) can, in principle, be accommodated by considering synchrotron self-absorption. This produces a relativistic Maxwellian distribution in the low-energy electrons (Ghisellini, Guilbert and Svensson 1988). The flattening of slope at the electron energy where synchrotron heating becomes ineffective causes the source function to rise faster than the $\nu^{2.5}$ of a pure-power law distribution (de Kool and Begelman 1989). The emission from a homogeneous source with a sharp edge could then rise as fast as $f_\nu \propto \nu^3$ over a decade in frequency as required by the observations.

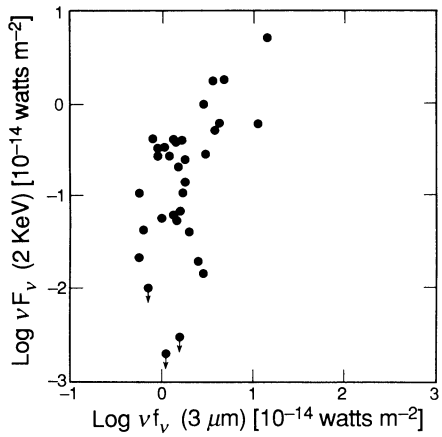

FIG. 9*a*

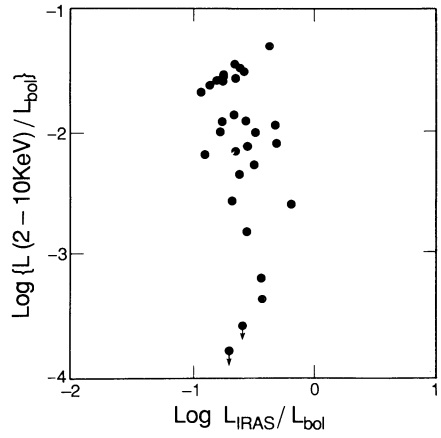

FIG. 9*b*

FIG. 9.—(*a*) X-ray flux (2–10 keV) vs. infrared flux at 3.5 μm for PG quasars. (*b*) X-ray luminosity fraction, $L_{(2-10\ \text{keV})}/L_{\text{bol}}$, versus infrared luminosity fraction, $L_{(2-100\ \mu\text{m})}/L_{\text{bol}}$, for PG quasars.

It would be surprising, however, if real sources, presumably coronae of accretion disks, were homogeneous and sharp-edged. Superposition of the emission from an inhomogeneous source gives spectra flatter than the local source functions. For example, suppose that the magnetic field strength in a corona scaled as $B \propto r^{-p}$, while the energy injected in particles per octave in radius scaled as r^{-q}. Then superposing emission from all radii gives, for a power-law electron spectrum, $\nu f_\nu \propto \nu^{3.5q/(q+2+p/2)}$, instead of the $\nu f_\nu \propto \nu^{3.5}$ local source function. Simple models give $q \simeq p \simeq 1$, and hence $f_\nu \propto \nu^0$. To get $f_\nu \propto \nu^2$ or steeper requires $p < 0$ unless $q > 12$, both of which seem rather unnatural.

The universality of the minimum in νf_ν at $10^{14.5}$ Hz (Neugebauer *et al.* 1987 and Fig. 1) furthermore requires in these models that the nonthermal flux in *all* sources be the same constant fraction of the thermal "blue bump" luminosity. This seems unusual, in light of the wide variability of the nonthermal emission in blazars and flat spectrum, radio-loud quasars.

VI. OBSERVATIONAL TESTS

The origin of the far-infrared and submillimeter continuum in quasars can ultimately be resolved by a measurement of the

brightness temperature. Nonthermal models are characterized by brightness temperatures $T_B \gtrsim 10^{10}$ K, while thermal models require $T_B \lesssim 10^2$ K. The two models thus predict angular sizes for the emitting region differing by a factor more than 10^4.

We show in Appendix B that an observation with a submillimeter interferometer with a baseline longer than 1 km would decide the issue. If a significant fraction of the flux is resolved, the emission is thermal; if it is not resolved, the emission is nonthermal. Likewise, if radio-quiet quasars were discovered to be rapidly variable at long wavelengths, causality arguments would require a small, and therefore nonthermal, emission region. Lack of variability is not sufficient to rule out nonthermal models, however. Appendix B also describes other ways to distinguish thermal from nonthermal emission.

VII. LUMINOSITY FUNCTIONS AND THEIR IMPLICATIONS FOR THE RELATION BETWEEN INFRARED AND ULTRAVIOLET-LOUD QUASARS

At short wavelengths the emergent spectrum of a quasar depends on whether or not the quasar is viewed through its dusty disk. The 60 and 100 μm fluxes, however, are probably optically thin, and therefore orientation independent. In this section, we use the 60 μm and bolometric luminosity functions to determine the distribution of covering factors by comparing the space densities of obscured and unobscured quasars.

a) 60 μm *Luminosity Function*

The 60 μm luminosity functions of the PG quasars, the *IRAS* Bright Galaxy Sample (Soifer *et al.* 1987) and the *IRAS* Warm Galaxy Sample (Sanders *et al.* 1988*b*) are presented in Figure 10. The *IRAS*–selected galaxies have the properties expected of PG quasars viewed through their dusty disk—they have 60 μm luminosities similar to those of PG quasars, but their 5–100 μm luminosity exceeds 80% of their bolometric luminosity. The local space density of these objects at all 60 μm luminosities is $\sim$100 times that of PG quasars (Fig. 10). As is evident from Figure 5*b*, the luminosity between 5 and 100 μm of the objects in the present UV–selected sample comprises 0.1–0.4 of the bolometric luminosity per unit solid angle emitted in the direction of Earth. If the central source emitted radiation isotropically, the covering factor of cool dust in PG quasars would have to be 0.1–0.4. It is difficult to imagine situations in which the dust opacity at 60 μm could be large, so we expect reradiation at 60 μm to be isotropic. Samples selected in that band will therefore be orientation-independent, so ratios of space densities at a given 60 μm luminosity correspond to ratios of covering factors, providing a test of unification schemes like that proposed by Barthel (1989). From Figure 10, it is evident that if *IRAS*–selected sources are quasars obscured by dust along the line of sight to the central source, the great majority of them must represent objects with much larger covering factors ($\sim$0.98) in dust than the PG, quasars. They could also, of course represent an entirely different class of object.

Except in the case that the narrow line gas is cospatial with the dusty disk in a symmetrical warp, it is difficult to prevent the narrow line region (NLR) from being visible from some viewing angles when the BLR is obscured. In our quasar model, this occurs for a fraction of sky of order the covering factor of the dust disk extending beyond the NLR: typically $\sim$0.05–0.1. Since molecular clouds are larger than the 0.1–1 pc

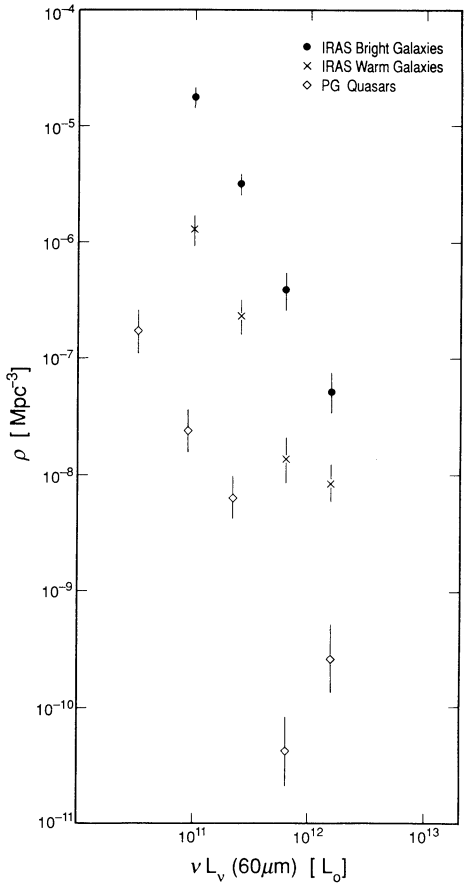

FIG. 10.—60 μm luminosity functions for PG quasars (this paper), *IRAS* bright galaxies (Soifer *et al.* 1987), and warm *IRAS* galaxies (Sanders *et al.* 1988*b*).

scale of the BLR, the same fraction of quasars with obscured broad-line regions would be expected even if the dust were in clouds at high latitudes rather than in a disk. These objects would appear as "quasar 2's" (by analogy to Seyfert 2 galaxies). Such objects have been rare in optical surveys, but appear commonly in infrared-selected samples (Sanders *et al.* 1988). In radio samples they may masquerade as narrow-line radio galaxies (Scheuer 1987).

In deciding what fraction of the *IRAS*-selected objects could be objects like the PG quasars, but viewed from an obscured angle, it should be borne in mind that the inner parts of the accretion disks in these high-luminosity objects may well be radiation pressure supported, and the UV radiation therefore substantially beamed along the axis of the accretion torus (Madau 1988). If this were the case, the ratio of the infrared to UV flux per unit solid angle in the direction of Earth in UV–selected objects would substantially underestimate the covering factor in cool dust, since off the axis of the inner disk the dust would see a much lower intensity of radiation than would the dust in completely enshrouded quasars with large infrared bumps. It is very implausible, however, that the anisotropy would be so extreme that only one line of sight in 100 would show an infrared excess. Unless the 60 μm flux is orientation dependent, which seems unlikely, the *IRAS* sources cannot differ from quasars only in viewing angle, as suggested by Barthel (1989).

b) Bolometric Luminosity

In Soifer *et al.* (1986, 1987), a bolometric correction of the form $L_{bol} = 9 \times \nu L_\nu(B)$ was applied to the blue luminosity of PG quasars to convert blue to bolometric luminosity. From the results derived in § III*b*, a more accurate representation of the bolometric luminosity of UV excess quasars is $L_{bol} = 16.5 \times \nu L_\nu(B)$. Thus Soifer *et al.* underestimated the contribution to the total luminosity of both the infrared and blue bumps. The steepness of the quasar luminosity function makes the comparison of space densities of objects depend sensitively on correct estimates of the frequency and solid angle integrated bolometric luminosities for different classes of objects.

The space density of UV excess quasars as a function of bolometric luminosity, taken from the work of Schmidt and Green (1983) converted to $H_0 = 75$ km s^{-1} Mpc^{-1} and using the new bolometric correction, is plotted with the space density of the *IRAS* samples displayed in Figure 11. The current bolometric correction for the UV excess quasars brings the space densities of the two classes of objects into closer agreement, although the density of infrared-selected, high-luminosity sources appears to exceed that of the UV quasars by a factor of 1.5–2.

Sanders *et al.* (1988*a*) have suggested that the relation between the ultraluminous infrared galaxies and UV-excess quasars is indeed one of covering factor. As argued above, the ultraluminous infrared galaxies must have a covering factor close to unity. The major difference between ultraluminous infrared galaxies and quasars may be the disruption or settling of the enshrouding dust cloud, allowing the central source to shine through. If this model is valid, and the luminosity does not vary between the two phases, Figure 11 suggests that the lifetime of the enshrouded infrared-bright phase of local quasars would be comparable to or slightly longer than the lifetime of the UV excess quasars.

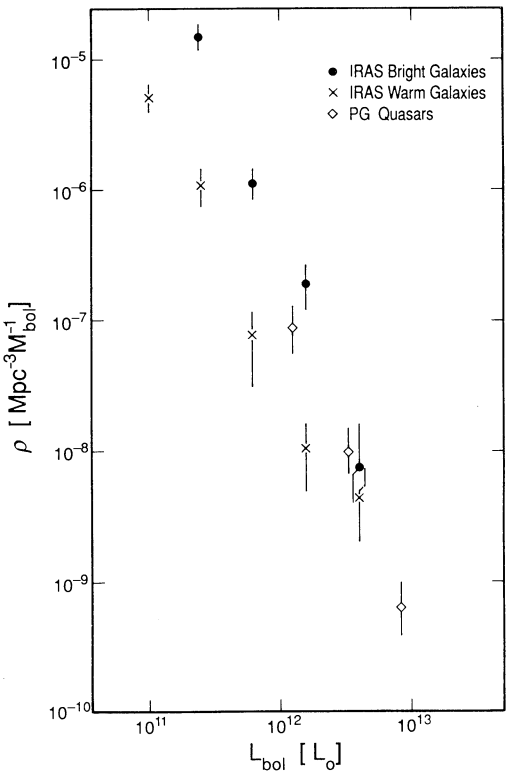

FIG. 11.—Bolometric luminosity functions for PG quasars (this paper), *IRAS* bright galaxies (Soifer *et al.* 1987), and warm *IRAS* galaxies (Sanders *et al.* 1988*b*).

VIII. SUMMARY

Continuum observations from 0.3 nm to 6 cm ($\sim 10^{9.7}$–10^{18} Hz) have been presented for 109 optically selected quasars from the Palomar-Green Bright Quasar Survey. It is now possible to give a fairly complete description of the shape of the infrared energy distribution and the nature of the infrared continuum from these quasars. Our analysis shows the following.

1. The far-infrared to soft X-ray continuum of radio-quiet and steep spectrum radio-loud PG quasars can be described by a model consisting of two broad peaks: an "infrared bump" at ~ 2 μm to 1 mm ($10^{11.5}$–$10^{14.2}$ Hz), and the well-known "big blue bump" at ~ 10 nm to 0.3 μm ($10^{15.5}$–10^{17} Hz). There is no obvious connection between the strengths of the infrared and blue peaks and whether the quasar is radio-quiet or radio-loud.

2. All PG quasars emit a significant fraction of their bolometric luminosity at infrared wavelengths ~ 1.5–100 μm. The fraction varies from 10% to 50% with a typical value of 30%. Most of the luminosity is typically emitted in the UV in the "big blue bump."

3. The ratio of the 6 cm flux density to that at 1 μm has a bimodal distribution and provides a discriminator at log $[\nu f_\nu(6\text{ cm})/\nu f_\nu(1\ \mu\text{m})] = -4$ between radio-loud and radio-quiet quasars.

4. There is no evidence for a tight correlation between the infrared and X-ray continua of quasars.

5. We suggest that the bulk of the emission between 2 μm and 1 mm in the infrared bump of the radio-quiet PG quasars and the radio-loud quasars with steep radio spectral indices is produced by thermal processes. It seems unavoidable that a nonnegligible fraction of the emission between 2 and 300 μm be due to thermal reradiation from a dusty disk which must be present in the host galaxies of most quasars. We interpret the radiation between 0.5 and 5 μm as reradiation from heated gas and dust in the outer edge of the accretion disk and in a disk of molecular gas within a few parsecs of the central source. The disk is shielded from direct radiation from the central source, but radiation will be scattered into the disk by the clouds of the broad-line region and any intercloud medium. We interpret the radiation from 5 μm to 1 mm as reradiation from dust in a warped disk extending from a few parsecs to a few kiloparsecs from the central source. The warping increases the effective covering factor of the disk more than a few parsecs from the central energy source, naturally producing the observed ratio of far-infrared to ultraviolet radiation.

6. The minimum in νf_ν near 1 μm is naturally explained as a result of the sudden change in disk temperature within 1 pc of the central source, when the equilibrium temperature rises above ~ 2000 K and the disks' dust sublimates. Within this radius, the disk emission at $10^{14.2}$–$10^{14.7}$ Hz is predominantly bremsstrahlung and naturally bridges the minimum in νf_ν.

7. The small range in the relative luminosities of the infrared and blue bumps suggests that the covering factor of dust in most of the PG quasars is similar, in the range 10%–30%.

8. The spectral index, $\alpha(f_\nu \propto \nu^\alpha)$ between 100 μm and 1 mm is nearly always larger than 2, suggesting that ~ 50 K dust emission determines the long wavelength cutoff of the infrared

bump. Such minimum temperatures are easily maintained by a central source heating dust within normal galaxy disks.

9. There is no convincing evidence for energetically significant nonthermal radiation in the wavelength range 10 nm to 300 μm (10^{12}–$10^{16.5}$ Hz) for radio-quiet and steep spectrum radio-loud PG quasars. Only the high-energy X-rays and the radio emission in these quasars require relativistic particles for their creation.

10. The 60 μm luminosity function shows that there are too many *IRAS* sources with quasar-like luminosities for these to be simply quasars like those in the PG sample, but viewed from their dust-obscured side. The majority of these *IRAS* sources must be completely obscured by dust, consistent with their generally steeper infrared spectra.

11. The luminosity function with corrected bolometric luminosities shows comparable space densities of UV bright quasars and infrared bright galaxies indicating that their lifetimes are comparable.

We thank Richard Green for providing us with the original data for the PG quasars and for helpful comments on the manuscript. We also thank our night assistants at Palomar, Juan Carasco and Skip Staples, for assistance in obtaining the infrared photometry. We acknowledge useful discussions with R. Blandford, and thank J. Bechtold and K. Kelleman for allowing us to use their data prior to publication. D. B. S., B. T. S., and G. X. N. are supported in part by the *IRAS* extended mission program. E. S. P. is supported in part by NSF PYI grant AST 84-51725 and the Irvine Foundation. Ground-based infrared astronomy at Caltech is supported by a grant from the NSF.

APPENDIX A

DATA FOR PG QUASAR ENERGY DISTRIBUTIONS

The data used to construct the PG quasar energy distributions displayed in Figure 1 are described below. Far-infrared data from *IRAS* and new, near-infrared measurements from Palomar are presented in Tables 2 and 3, respectively. Data in other bands have been taken from the literature.

a) Radio (~21 cm–2 cm)

Six centimeter measurements have been taken from the recent survey of (Kellerman *et al.* 1989). All but four PG quasars were observed with the VLA at 6 cm, and all but four of the sources observed were detected. Multiwavelength measurements for 15 of the 20 radio-loud quasars have been taken from Kühr *et al.* (1981). VLA measurements at 21 cm and 2 cm for eight radio-quiet quasars have been taken from Antonucci and Barvainis (1988*a*, *b*).

b) Millimeter

Data for 30 PG quasars at ~1.25 mm have been taken from Chini, Kreysa, and Biermann (1988) and Keene *et al.* (1988). Only six (of 30) sources have been detected. For the remaining sources, the measured upper limits are typically 5–20 mJy (3 σ). Measurements at 1 mm and 3 mm for PG 1634+706 are from Antonucci and Barvainis (1988*b*). The 1 mm measurement for PG 0007+10 is from Ennis, Neugebauer, and Werner (1982).

c) Submillimeter

There are almost no published submillimeter measurements of PG quasars except for the radio-loud quasar 3C 273. Submillimeter data for 3C 273 are taken from Clegg *et al.* (1983). Observations at 150 and 370 μm have recently been reported for the radio-quiet quasar PG 0050+124 (Engargiola *et al.* 1988) indicating a fairly rapid turnover in the continuum energy distribution beyond 100 μm as shown in Figure 1.

d) Far-infrared

Table 2 presents *IRAS* measurements for 107 of the 109 objects in the PG sample. PG 1116+215 and PG 2209+184 were in the small portion of the sky not surveyed by *IRAS* data were obtained at various times throughout 1983. Fifty-eight sources (54%) were detected in one or more of the four *IRAS* bands at 12, 25, 60, or 100 μm. Column (6) indicates whether the data were obtained from the more sensitive *IRAS* pointed observations, many of which were reported earlier by Neugebauer *et al.* (1986), or from co-adding survey data.

Typically, a single pointed observation sequence was five times more sensitive than the survey for a point source. The flux densities of the PG quasars not observed in the pointed observations were determined by two different reduction algorithms for combining the various *IRAS* survey scans—the ADDSCAN and DSGAD algorithms. When the source has a signal which is near to the noise level, the results of both algorithms are subjective due to the intrinsic faintness of the source, confusion by nearby galaxies or "infrared cirrus" (Low *et al.* 1984). We have arbitrarily selected the procedure that when the quasar was clearly detected in one band with a signal-to-noise ratio greater than 3, that detections in accompanying bands with lower signal to noise ratios be indicated with the appendage semicolon (:). The observations so indicated are of very low, even dubious quality and might well be considered as limits. The semicolon appendage is considered appropriate since the uncertainties for these sources are uncertain and subjective. Survey coadds are, in general only a factor of 3 more sensitive than the sensitivity limits of the all-sky survey for point sources (5 $\sigma \simeq$ 0.5 Jy at 12, 25, and 60 μm and 1.5 Jy at 100 μm). The *IRAS* survey and pointed observations have been described in detail in the *IRAS Explanatory Supplement* (1985), and in Young *et al.* (1985), respectively.

Figure 12 presents data needed to determine whether the sources not detected by *IRAS* represent a distinct population of quasars

TABLE 2

IRAS FLUX DENSITIES OF PG BRIGHT QUASARS

Object (PG)	12μm	25μm	60μm	100μm	Z	log $\nu f_{14.5}$ (w m^{-2}) [a]	Notes [b]	Notes [c]
	(mJy)							
0002+051	<112	<148	<170	<380	1.900	-14.29	SC	L
0003+158	<36	<86	<67	<187	0.450	-14.09	PO	L
0007+106	99±6	163±12	213±8	<845	0.089	-13.70	PO	L,F
0026+129	<18	<40	<27	<80	0.142	-14.01	PO	Q
0043+039	<117	<182	<170	<347	0.348	-14.26	SC	Q
0044+030	<123	<182	<348	<380	0.624	-14.35	SC	L
0049+171	<110	<132	<155	<380	0.064	-14.09	SC	Q
0050+124	549±11	1097±20	2293±17	2959±51	0.061	-13.30	PO	Q,S
0052+251	<80	<180	93±18	<338	0.155	-14.09	PO	Q
0117+213	<110	<132	<170	<347	1.493	-14.60	SC	Q
0157+001	137±38	520±58	2377±56	2322±130	0.164	-14.07	PO	Q,S
0804+761	190±27	209±27	191±42	<315	0.100	-13.70	SC	Q
0832+251	<94	<153	<126	<284	0.320	-14.12	SC	—
0838+770	34±5	103±7	174±9	426±30	0.131	-14.25	PO	Q
0844+349	126±29	204±40	163±41	294±97	0.064	-13.82	PO	Q
0906+484	39±6	87±8	172±10	291±32	0.118	-14.30	PO	Q
0923+201	<98	<153	<300	<1000	0.190	-14.06	SC	Q[d]
0931+437	<89	149±33	210:	<347	0.457	-14.59	SC	—
0935+417	<89	<100	<126	<315	1.980	-14.22	SC	—
0946+301	<94	<133	<140	<315	1.216	-14.27	SC	Q
0947+396	<91	90:	201±47	462±105	0.206	-14.57	SC	Q
0953+414	<89	<107	<129	<315	0.239	-14.10	PO	Q
1001+054	31±6	36±12	27±9	<69	0.161	-14.30	PO	Q
1004+130	<91	150:	191±42	<284	0.240	-14.17	SC	L
1008+133	130:	178±56	<140	<315	1.280	-14.80	SC	Q
1011-040	<87	<113	163±42	<252	0.058	-13.80	SC	Q
1012+008	<108	<147	<140	<347	0.185	-14.25	SC	Q
1048+342	<94	<107	<140	<347	0.167	-14.25	SC	Q
1048-090	<110	<127	<154	<378	0.344	-14.28	SC	L
1049-005	90:	180±53	191±56	<410	0.357	-14.33	SC	Q
1100+772	17±5	45±6	61±9	<85	0.313	-14.21	PO	L,S
1103-006	<117	<153	130±51	<388	0.425	-14.48	SC	L
1112+431	<89	80:	182±47	<315	0.302	-14.92	SC	—
1114+445	110:	149±33	191±47	<347	0.144	-14.14	SC	Q
1115+080	<117	<160	<1000	<1000	1.722	-14.17	SC	Q[e]
1115+407	<91	<100	<140	<347	0.154	-14.28	SC	Q
1116+215	—	—	—	—	0.177	-13.74	SC	Q
1119+120	120±40	280±53	546±51	746±126	0.049	-13.82	SC	Q
1121+422	<87	<93	<140	<315	0.234	-14.38	SC	Q
1126-041	104±19	309±35	669±26	1172±134	0.060	-13.63	PO	Q
1138+040	<117	<180	<140	<347	1.876	-14.80	SC	Q
1148+549	<75	120±24	196±42	410±105	0.969	-14.30	SC	Q
1151+117	<112	<160	<154	<347	0.176	-14.21	SC	Q
1202+281	<98	124±38	110:	420±105	0.165	-14.31	SC	Q
1206+459	207±36	<113	250:	<1000	1.158	-14.38	SC	Q[e]
1211+143	172±38	362±51	305±53	689±119	0.085	-13.60	PO	L,S
1216+069	<115	<173	<154	<315	0.334	-13.99	SC	Q
1222+228	<110	<120	<140	<347	2.046	-14.06	SC	L

TABLE 2—*Continued*

Object (PG)	12μm	25μm	60μm	100μm	Z	log $\nu f_{14.5}$ (w m^{-2}) [a]	Notes [b]	Notes [c]
	(mJy)							
1226+023	417±12	941±27	1805±14	3109±45	0.158	-13.02	PO	L,F
1229+204	117:	302±38	163±42	<462	0.064	-13.74	SC	Q
1241+176	<108	<140	<154	<315	1.273	-13.85	SC	L
1244+026	<117	100:	280±51	<315	0.048	-14.14	SC	Q
1247+267	<126	<113	<140	<315	2.038	-13.91	SC	Q
1248+401	<117	<200	224±51	<378	1.030	-14.59	SC	Q
1254+047	<115	<160	<154	<347	1.024	-14.25	SC	Q
1259+593	<112	<120	<154	<347	0.472	-14.16	SC	Q
1302-102	<119	<180	<168	<410	0.286	-13.87	SC	L,F
1307+085	<112	<153	<154	<347	0.155	-14.10	SC	Q
1309+355	<101	<100	<140	<347	0.184	-14.12	SC	L
1310-108	<117	<187	<154	<378	0.035	-13.80	SC	Q
1322+659	<72	<59	<89	<257	0.168	-14.12	SC	Q
1329+412	<105	<100	<140	<347	1.930	-14.69	SC	Q
1333+176	<84	<80	<140	<378	0.554	-14.31	SC	A
1338+416	113±33	80:	<140	<347	1.219	-14.37	SC	Q
1351+236	<105	<113	364±51	420±105	0.055	-13.75	SC	Q
1351+640	173±5	532±6	757±8	1184±26	0.087	-13.86	PO	Q,S
1352+183	<105	<113	<140	<347	0.158	-14.10	SC	Q
1352+011	<110	<160	<154	<347	1.121	-14.30	SC	Q
1354+213	<105	<113	<154	<347	0.300	-14.54	SC	Q
1402+261	70:	<107	229±51	340:	0.164	-14.10	SC	Q
1404+226	<103	<100	<154	<347	0.098	-14.22	SC	Q
1407+265	<206	<100	<140	<347	0.944	-14.27	SC	L
1411+442	115±10	160±12	162±17	<175	0.089	-13.87	PO	Q
1415+451	80:	70:	112±37	260:	0.114	-14.04	SC	Q
1416-129	<108	<180	<140	<315	0.129	-13.90	SC	Q
1425+267	<93	<85	<115	<316	0.366	-14.35	SC	L
1426+015	124±33	171±46	318±47	<315	0.086	-13.77	PO	Q
1427+480	<75	<73	<112	<252	0.221	-14.47	SC	Q
1435-067	<96	<153	<126	<315	0.129	-14.00	SC	Q
1440+356	98±13	208±15	652±21	1061±64	0.077	-13.70	PO	Q,S
1444+407	<82	107±24	117±39	170:	0.267	-14.28	SC	Q
1448+273	70:	120±24	117±37	<252	0.065	-13.81	SC	Q
1501+106	109±29	431±33	486±42	<284	0.036	-13.54	SC	Q
1512+370	<38	<42	61±20	<178	0.371	-14.44	PO	L,I
1519+226	<73	<73	<112	<252	0.137	-14.09	SC	Q
1522+101	<89	<100	<126	<284	1.321	-14.55	SC	Q
1534+580	99±24	182±22	160:	300:	0.030	-13.78	SC	Q
1535+547	108±27	118±24	<126	<568	0.038	-13.59	SC	Q
1543+489	58±15	126±18	348±26	485±79	0.400	-14.52	PO	Q
1545+210	<31	<37	<50	<141	0.266	-14.05	PO	L,S
1552+085	105±30	<100	<126	<315	0.119	-14.26	SC	Q
1612+261	<33	<40	<54	<161	0.131	-14.12	PO	Q
1613+658	87±12	231±14	635±19	1090±59	0.129	-13.97	PO	Q,I
1617+175	<68	<67	<98	<252	0.114	-13.95	SC	Q
1626+554	<38	<39	<70	<238	0.133	-14.19	PO	Q
1630+377	<75	<67	<112	<284	1.471	-14.27	SC	Q

TABLE 2—*Continued*

Object (PG)	12μm	25μm	60μm	100μm	z	log $\nu f_{14.5}$ (w m^{-2}) [a]	Notes b	Notes c
	(mJy)							
1634+706	61±13	147±14	318±23	343±72	1.334	-14.00	PO	Q,F
1700+518	120±23	220±21	480±36	482±88	0.292	-13.90	PO	Q,S
1704+608	46±5	125±5	183±9	<299	0.371	-14.18	PO	L,S
1718+481	<81	<66	<107	<309	1.084	-14.10	SC	L
2112+059	71±13	73±25	105±19	<177	0.466	-14.08	PO	Q
2130+099	186±9	380±10	479±12	<1000	0.061	-13.71	SC	Q,I
2209+184	—	—	—	—	0.070	-13.81	SC	L,F
2214+139	61±7	95±12	337±11	<282	0.067	-13.70	PO	Q,S
2233+134	<105	<113	<154	<1000	0.325	-14.60	SC	Q
2251+113	<36	<66	<67	<214	0.323	-13.93	PO	L,S
2302+029	<107	<123	<126	<331	1.044	-14.49	SC	Q
2344+092	<19	71±13	67±8	<135	0.677	-14.55	PO	L,F
2349-014	<119	<180	271±51	290:	0.174	-14.00	SC	L,I

[a] Rest frame νf_ν (±0.05), at log ν = 14.5 Hz.
[b] SC = survey coadd; PO = pointed observation.
[c] Q = radio quiet; L = radio loud; *F* = flat radio spectrum; S = steep radio spectrum; I = intermediate radio spectrum.
[d] Confusion with infrared cirrus.
[e] Confusion with nearby galaxy.

with intrinsically weaker far-infrared emission as opposed to a more distant population of quasars with similar far-infrared properties. Figure 12*a* compares the redshift distributions for both detected and nondetected PG quasars; the sources not detected in the far-infrared have a mean redshift a factor 2.2 larger than the detected sources. Figure 12*b* shows that the mean strength of the far-infrared bump for the detected sources, as measured by the ratio of the 25 to 1 μm flux densities, is a factor of $\sim$3 less than the upper limit at 25 μm for the nondetected sources. The infrared energy distributions of upper limits are consistent with the distribution of detections. Therefore, it seems reasonable to assume that both the sources detected and not detected by *IRAS* have similar far-infrared properties.

e) Near-infrared

Extensive near-infrared observations of PG quasars have previously been published by Neugebauer *et al.* (1987), including measurements at *J* (1.27 μm), *H* (1.65 μm), and *K* (2.2 μm) of all objects, and measurements at *L*′ (3.7 μm) and *N* (10.1 μm) for approximately one-third of the sample. Table 3 gives new infrared measurements at 3.7 and 10.1 μm obtained with the Palomar 5 m telescope. At 3.7 μm the beam diameter was typically 5″, and observations at 10.1 μm were always made with a beam diameter of

TABLE 3

NEW MEASUREMENTS AT 3.7 AND 10.1 μm

OBJECT (PG)	f_ν (mJy) 3.7 μm	f_ν (mJy) 10.1 μm	DATE
0002+051	1.80 ± 0.36	<13.5	1986 Sep 20
0049+171	3.66 ± 0.63	...	1987 Sep 3
0050+124	127. ± 0.08	431. ± 0.47	1987 Sep 4
0923+201	14.7 ± 0.12	...	1987 Apr 9
0931+437	7.05 ± 0.78	...	1987 Apr 9
1116+215	32.5 ± 0.24	...	1986 Jan 24
1126−041	24.7 ± 0.18	...	1987 Apr 10
1202+281	11.2 ± 0.08	34.5 ± 0.75	1987 Mar 9
1307+085	12,4 ± 0.09	26.4 ± 0.64	1987 Mar 9
1425+267	9.12 ± 1.15	<42.7	1988 Mar 29
1512+370	5.11 ± 0.70	15.2 ± 0.45	1986 May 19
1535+547	37.0 ± 0.31	72.1 ± 0.06	1986 May 18
1543+489	7.52 ± 1.03	34.2 ± 0.68	1987 Sep 5
1552+085	6.79 ± 0.75	<33.0	1987 Sep 6
1630+377	2.54 ± 0.55	...	1986 Apr 23
2214+139	20.7 ± 0.13	...	1986 Oct 20
2233+134	6.25 ± 0.08	21.6 ± 0.49	1987 Sep 4
2344+092	3.94 ± 0.72	22.6 ± 0.63	1987 Sep 6
2349−014	20.0 ± 0.13	22.0 ± 0.77	1987 Sep 4

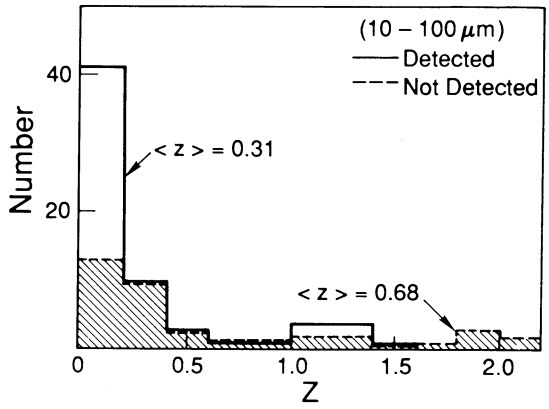

FIG. 12*a*

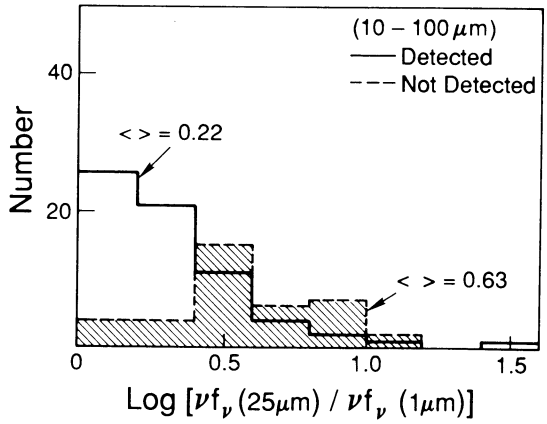

FIG. 12*b*

FIG. 12.—(*a*) Comparison of redshift distributions for PG quasars detected and not detected at wavelengths 10 to 100 μm. (*b*) The strength of the infrared peak as measured by the ratio $vf_\nu(25\ \mu m)/vf_\nu(1\ \mu m)$, of PG quasars detected at wavelengths 10 to 100 μm compared to the upper limit for the strength of the infrared peak using the upper limit for $vf_\nu(25\ \mu m)$ for PG quasars not detected at wavelengths 10–100 μm.

4″.6. The uncertainties in the measurements at 3.7 μm are typically 6%–10%; at 10.1 μm, the uncertainties were typically 15%. The 3.7 and 10.1 μm measurements were always accompanied by observations in the standard infrared bands *J*, *H*, and *K*. Including these new data, 72 PG quasars have now been observed at *L*′, and 65 PG quasars have been observed at *N* with the Palomar 5 m telescope.

The agreement between the *IRAS* 12 μm measurements and the ground-based 10 μm measurements from Palomar is, in general, quite good. For sources detected not only at 10 and 12 μm, but at 3.7 and 25 μm as well, a smooth curve can be drawn through the data as shown in Figure 1*a*. In a few cases, a dashed curve is used instead to represent that portion of the far-infrared energy distribution where there was some ambiguity in how steeply the distribution turned over, usually at the longer wavelengths, or where *IRAS* upper limits seemed to indicate small, but abrupt changes in the shape of the distribution.

f) *Optical*

The visual continua 0.32–0.84 μm for all of the PG quasars were measured at the Palomar 5 m telescope using a multichannel spectrophotometer as described in Neugebauer *et al.* (1987). Observations for all of the objects were obtained over a 2 month period in 1980. In all cases a focal-plane diaphragm of 15″ diameter was used. The data used in Figure 1 are taken directly from Neugebauer *et al.* (1987), and therefore include corrections for Galactic extinction and for removal of spectral lines.

g) *Ultraviolet*

At wavelengths 0.1 to 0.3 μm data for 15 PG quasars have been taken from Elvis *et al.* (1986), and Bechtold *et al.* (1987). No data are available in the far UV (0.01–0.1 μm). However, it is clear from the soft X-ray data that the energy distributions of most PG quasars must drop by almost an order of magnitude between ~0.01 and 0.1 μm.

h) *X-ray*

X-ray data at ~0.2 to 4 keV are available for nearly half of the PG sources. Measurements at 2 keV have been taken from Tananbaum *et al.* (1986), Elvis *et al.* (1986), and Bechtold *et al.* (1987). Additional 1 keV measurements, as well as mean X-ray spectral indices for radio-loud and radio-quiet quasars, have been taken from Wilkes and Elvis (1987). X-ray data for PG 0026+129 are from Treves *et al.* (1988).

APPENDIX B

ANGULAR SIZE MEASUREMENTS: THERMAL VERSUS NONTHERMAL

Synchrotron models for the far-infrared and submillimeter continuum require brightness temperatures exeeding $m_e c^2/k \sim 10^{10}$ K, and thus in quasars predict angular sizes of the order of microarcseconds. As we now show, however, thermal models predict angular sizes of fractions of 1″, accessible to the next generation of submillimeter interferometers. An absolute lower limit to the angular sizes for thermal models in the blackbody limit, which at submillimeter wavelengths, where temperatures of ~ 100 K are appropriate (§ IV*c*[i]), is typically $\theta \gtrsim 0\farcs02$ for the PG quasars. A definitive resolution of the present controversy over the nature of the far-infrared and submillimeter flux from radio-quiet quasars is thus within reach.

We can estimate the angular size θ of a distribution of dust at temperature T_d in two ways. First, assume the observed dust lies at distance $r = D_A\theta$ from a central source of luminosity L_c, behind an optical depth τ; D_A is the angular diameter distance to the source. The (absorption-corrected) total flux from the source at Earth is $F = L_c/[4\pi D_A^2(1+z)^4]$. Then the angular radius of the dust must be

$$\theta = \left[\frac{(1+z)^4}{\sigma T_d^4}\frac{F e^{-\tau}}{4}\frac{\langle Q_a\rangle}{\langle Q_e\rangle}\right]^{1/2}, \tag{B1}$$

where σ, $\langle Q_e\rangle$ and $\langle Q_a\rangle$ are as defined in § IV*b*. Typically $\langle Q_a\rangle/\langle Q_e\rangle \simeq 10^3\lambda_{100}/(1+z)$, where $\lambda_{100} = \lambda/100$ μm and λ is the observing wavelength. For the sources in our sample, the predicted angular size at submillimeter wavelengths is then typically $\sim 1''$, resolvable with a baseline of $20\lambda_{100}$ m.

An independent lower limit to the angular size θ permitted by thermal emission at the observing frequency ν follows by noting that the flux density observed at the Earth is given by

$$f_\nu = \int d^2\Omega\, B_\nu\left(\frac{T_d}{1+z}\right)(1-e^{-\tau_\nu}) \simeq \pi\theta^2 f_c\left\langle B_\nu\left(\frac{T_d}{1+z}\right)(1-e^{-\tau_\nu})\right\rangle, \tag{B2}$$

where $B_\nu[T_d/(1+z)]$ is the Planck function, f_c is the sky covering factor if the dust is clumpy, and τ_ν is the optical depth at the observing frequency integrated along a given line of sight through the source. The average is over lines of sight.

The optical depth may be approximated by $\tau_\nu = Q_a[\nu(1+z)]\tau_g$, where $Q_a[\nu(1+z)]$ is the absorption efficiency of the intervening dust, and τ_g is the geometrical optical depth along the line of sight (roughly the optical depth for absorption of ultraviolet photons from the central source). If, as appropriate at submillimeter wavelengths, the intervening material is optically thin and the Rayleigh-Jeans limit applies, equation (B2) becomes

$$f_\nu \simeq 2000\left(\frac{T_{100}}{1+z}\right)\left(\frac{\theta_{11}}{\lambda_{100}}\right)^2 f_c\langle Q_a[\nu(1+z)]\rangle\tau_g \text{ Jy}, \tag{B3}$$

where T_{100} is the temperature T_d in units of 100 K of the dust which contributes most to the submillimeter flux (see § IV*c*[i], and θ'' is the angular diameter in arcseconds. $\langle Q_a(\nu)\rangle$ depends on the dust's composition and size distribution; for local Galactic dust $\langle Q_a[\nu(1+z)]\tau_g\rangle \approx 1.3\times 10^{-3}\lambda_{100}^{-1}(1+z)A_v$ (Draine and Lee 1984). Our thermal models require $f_c A_v \gtrsim 0.1$. A disk packed with molecular cloud cores would have $(\Omega/4\pi)A_v \lesssim 10$. For a thermal source with a flux density $f_\nu(100)$ Jy at 100 μm, then $\theta \gtrsim 0\farcs2 f_\nu(100)^{1/2}$.

There are several additional experiments whose outcomes could strengthen the case for either thermal or nonthermal emission:

Monitoring over time the flux from radio-quiet quasars at frequencies $10^{11.5}$–$10^{12.6}$ Hz could rule out thermal models if, for instance, the flux varied by more than 50% on time scales shorter than 5 yr. Although a nonthermal contribution could vary on time scales as short as hours, a thermal contribution should not vary by factors of 2 on time scales much shorter than the light-crossing time, $t_{\rm cross}$, to the dust radiating at the observing frequency. At a frequency $\nu = 10^{14}\nu_{14}$ Hz, $t_{\rm cross} \sim \nu_{14}^{-2}(\nu L_\nu/10^{12}\ L_\odot)^{1/2}$ yr. This seems consistent with the observation that the variability at 1–3 μm in most active galactic nuclei appears to be much more pronounced than that at wavelengths greater than 10 μm (Rieke and Lebofsky 1981; Rieke 1985; Cutri *et al.* 1985; Edelson and Malkan 1987; see also discussion in Neugebauer *et al.* 1989), and may show the expected time lags relative to continuum variations (Clavel *et al.* 1989). Detection of variability violating these constraints would indicate that the variable component of flux was nonthermal. Nondetection of variability, does not, however, rule out nonthermal models, so this test is not as clean as the interferometer measurements.

Measurement of large ($\gtrsim$30%) or variable polarization in the infrared would also hint at a nonthermal source, since dust scattering and transmission does not typically produce very large polarization. Absence of a large polarization would not disprove nonthermal models, however, since the emission could be depolarized or originate in a region without ordered magnetic fields.

Likewise, measurement of the silicate emission features at 9.7 and 18 μm, or of the emission from polycyclic aromatic hydrocarbons (PAH—3.3, 7.7, 8.6, and 11.3 μm; Allamandola, Tielens, and Barker 1985; Puget, Léger, and Boulanger 1985) would clearly indicate a thermal origin for much of the infrared emission (Kleinmann, Gillett, and Wright 1976; Willner *et al.* 1977; Roche and Aitken 1985). However, absence of such features (Aitken and Roche 1985) does not disprove a thermal model. Most of the $\lambda < 12$ μm infrared emission in quasars could come from large, continuously hot grains, rather than from small quantum-heated grains present in the reflection nebulae and starburst galaxies which show the PAH emission features. The 3.3, 8.6, and 11.3 μm features, due to C—H stretch and bending (Léger and d'Hendecourt 1987) would also be absent if UV heating were so severe that the small grains did not have significant amounts of adsorbed hydrogen.

REFERENCES

Aitken, D. K., and Roche, P. F. 1985, *M.N.R.A.S.*, **213**, 777.
Allamandola, L. J., Tielens, A. L. G. M., and Barker, J. R. 1985, *Ap. J. (Letters)*, **290**, L25.
Antonucci, R. R. J., and Barvainis, R. 1988*a*, *Ap. J. (Letters)*, **325**, L21.
———. 1988*b*, *Ap. J. (Letters)*, **332**, L13.
Antonucci, R. R. J., and Miller, J. S. 1985, *Ap. J.*, **297**, 621.
Backer, D. C., *et al.* 1987, *Ap. J.*, **322**, 74.
Band, D. L. 1987, *Ap. J.*, **321**, 80.
Barthel, P. 1989, *Ap. J.*, **336**, 606.
Barvainis, R. 1987, *Ap. J.*, **320**, 537.
Bechtold, J., Czerny, B., Elvis, M., Fabbiano, G., and Green, R. F. 1987, *Ap. J.*, **314**, 699.
Becklin, E. E., and Wynn-Williams, C. G. 1987, in *Star Formation in Galaxies*, ed. C. J. Lonsdale (NASA CP2466), p. 643.
Blandford, R. D. 1987, in *Superluminal Radio Sources*, ed. J. A. Zensus, and T. J. Pearson (Cambridge: Cambridge University Press), p. 310.
Blandford, R. D., and Königl, A. 1979, *Ap. J.*, **232**, 34.
Bollea, D., and Cavaliere, A. 1976, *Astr. Ap.*, **49**, 313.
Bosma, A. 1983, in *Internal Kinematics and Dynamics of Galaxies*, ed. E. Athanassoula (Dordrecht: Reidel), p. 11.
Carieton, N. P., Elvis, E., Fabbiano, G., Willner, S. P., Lawrence, A., and Ward, M. 1987, *Ap. J.*, **318**, 595.
Chini, R., Kreysa, E., and Biermann, P. L. 1988, *Astr. Ap.* preprint.
Clavel, J., Wamsteker, W., and Glass, I. S. 1989, *Ap. J.*, **337**, 236.
Clegg, R. E. S., *et al.* 1983, *Ap. J.*, **273**, 58.
Collin-Souffrin, S. 1987, *Astr. Ap.*, **179**, 60.
Condon, J. J. 1980, *Ap. J.*, **242**, 894.
Courvoisier, T. J-L., Robson, E. I., Hughes, D. H., Blecha, A., Bouchet, P., Krisciunas, K., and Schwarz, H. E. 1988, preprint.
Curti, R. M., Wisniewski, W. Z., Rieke, G. H., and Lebofsky, M. J. 1985, *Ap. J.*, **296**, 423.
Czerny, B., and Elvis, M. 1987, *Ap. J.*, **321**, 305.
de Bruyn, A. G., and Wilson, A. S. 1976, *Astr. Ap.*, **53**, 93.
de Jong, T., Klein, U., Wielebinski, R., and Wunderlich, E. 1985, *Astr. Ap.*, **147**, L6.
de Kool, M., and Begelman, M. C. 1989, *Nature*, **338**, 484.
Draine, B. T. 1981, *Ap. J.*, **245**, 880.
Draine, B., and Lee, H. M. 1984, *Ap. J.*, **285**, 89.
Edelson, R. A., Gear, W. K. P., Malkan, M. A., and Robinson, E. I. 1988, *Nature*, **336**, 749.
Edelson, R. A., and Malkan, M. A. 1986, *Ap. J.*, **308**, 59.
———. 1987, *Ap. J.*, **323**, 516.
Elvis, M., Green, R. F., Bechtold, J., Schmidt, M., Neugebauer, G., Soifer, B. T., Matthews, K., and Fabbiano, G. 1986, *Ap. J.*, **310**, 291.
Engargiola, G., Harper, D. A., Elvis, M., and Willner, S. P. 1988, *Ap. J. (Letters)*, **332**, L19.
Ennis, D. J., Neugebauer, G., and Werner, M. 1982, *Ap. J.*, **262**, 460.
Ferland, G. J. 1981, *Ap. J.*, **249**, 17.
Ferland, G. J., and Shields, G. A. 1985, in *Astrophysics of Active Galaxies and Quasi-Stellar Objects*, ed. J. S. Miller, (Millvalley, CA: University Science Books), p. 157.
Fitt, A. J., Alexander, P., and Cox, M. J. 1988, preprint.
Gavazzi, G., Cocito, A., and Vettolani, G. 1986, *Ap. J. (Letters)*, **305**, L15.
Gear, W. K., Gee, G., Robson, E. I., Ade, P. A. R., and Duncan, W. D. 1986*a*, *M.N.R.A.S.*, **219**, 19P.
Gear, W. K., Gee, G., Robson, E. I., and Nolt, I. G. 1985, *M.N.R.A.S.*, **217**, 281.
Gear, W. K., *et al.* 1986*b*, *Ap. J.*, **304**, 295.
Genzel, R., and Townes, C. H. 1987, *Ann. Rev. Astr. Ap.*, **25**, 377.
Ghisellini, G., Guilbert, P. W., and Svensson, R. 1988, *Ap. J. (Letters)*, **334**, L5.
Green, R. F., Schmidt, M., and Liebert, J. 1986, *Ap. J. Suppl.*, **61**, 305.
Haniff, C. A., Wilson, A. S., and Ward, M. J. 1988, preprint.
Helou, G., Soifer, B. T., and Rowan-Robbinson, M. 1985, *Ap. J. (Letters)*, **298**, L7.
Hummel, E. 1981, *Astr. Ap.*, **93**, 93.
Hutchings, J. B. 1983, *Pub. A.S.P.*, **95**, 799.
Hyland, A. R., and Allen, D. A. 1982, *M.N.R.A.S.*, **199**, 943.
Hyland, A. R., Becklin, E. E., and Neugebauer, G. 1978, *Ap. J. (Letters)*, **220**, L73.
Impey, C. D., and Neugebauer, G. 1988, *A.J.*, **95**, 307.
IRAS Explanatory Supplement. 1985, ed. C. A. Beichman, G. Neugebauer, H. J. Habing, P. E. Clegg, and T. J. Chester (Washington, DC: US GPO).
Jura, M. 1982, *Ap. J.*, **254**, 70.
Kallman, T. R., and Krolik, J. H. 1986, *Ap. J.*, **308**, 805.
Keene, J., Neugebauer, G., Carcio, D., Sanders, D., and Soifer, T. 1988, in *Active Galactic Nuclei*, ed. J. Miller and D. Osterbrock, in press.
Kellermann, K. I., Sramek, R., Shaffer, D. Green, R. F., and Schmidt, M. 1989, in preparation.
Kleinmann, D. E., Gillett, F. C., and Wright, E. L. 1976, *Ap. J.*, **208**, 42.
Kriss, G. A. 1988, *Ap. J.*, **324**, 809.
Krolik, J. H., and Begelman, M. C. 1988, *Ap. J.*, **329**, 702.
Krolik, J. H., McKee, C. F., and Tarter, C. B. 1981, *Ap. J.*, **249**, 422.
Kühr, H., Witzel, A., Pauliny-Toth, I. I. K., and Nauber, U. 1981, *Astr. Ap. Suppl.*, **45**, 367.
Léger, A., and d'Hendecourt, L. 1987, in *Polycyclic Aromatic Hydrocarbons and Astrophysics*, ed. A. Léger *et al.* (Dordrecht: Reidel), p. 223.
Low, F. J., Cutri, R. M., Kleinmann, S. G., and Huchra, J. P. 1989, *Ap. J. (Letters)*, **340**, L1.
MacKenty, J. W., and Stockton, A. 1984, *Ap. J.*, **283**, 64.
Madau, P. 1988, *Ap. J.*, **327**, 116.
Malkan, M. A. 1984, in *X-ray and UV Emission from Active Galactic Nuclei*, ed. W. Brinkmann and S. Trümper (MPIfR), p. 121.
Malkan, M. A., and Sargent, W. L. W. 1982, *Ap. J.*, **254**, 22.
Mathis, J. S., Rumpl, W., and Nordsieck, K. H. 1977, *Ap. J.*, **217**, 425.
McAlary, C. W., and Rieke, G. H. 1988, *Ap. J.*, **333**, 1.
Neugebauer, G., Green, R. F., Matthews, K., Schmidt, M., Soifer, B. T., and Bennett, J. 1987, *Ap. J. Suppl.*, **63**, 615.
Neugebauer, G., Matthews, K., Soifer, B. T., and Elias, J. H. 1985, *Ap. J.*, **298**, 275.
Neugebauer, G., Miley, G. K., Soifer, B. T., and Clegg, P. E. 1986, *Ap. J.*, **308**, 815.
Neugebauer, G., Oke, J. B., Becklin, E. E., and Matthews, K. 1979, *Ap. J.*, **230**, 79.
Neugebauer, G., Soifer, B. T., Matthews, K., and Elias, J. H. 1989, *A.J.*, **97**, 957.
Neugebauer, G., *et al.* 1984, *Ap. J. (Letters)*, **278**, L83.
Norris, R. P. 1985, *M.N.R.A.S.*, **216**, 701.
Norris, R. P., Kesteven, M. J., Allen, D. A., and Troupe, E. 1988, *M.N.R.A.S.*, **234**, 51P.
Novikov, I. D., and Thorne, K. S. 1973, in *Black Holes—Les Astres Occlus*, ed. C. De Witt and B. S. De Witt (New York: Gordon & Brech), p. 13.
Phinney, E. S. 1983, Ph.D. thesis, University of Cambridge.
———. 1989*a*, in *IAU Symposium 136, The Center of the Galaxy*, ed. M. Morris (Dordrecht: Kluwer), p. 543.
———. 1989*b*, in preparation.
———. 1989*c*, in *Theory of Accretion Disks*, ed. W. Duschl *et al.* (Dordrecht: Kluwer), in press.
Puetter, R. C., and Hubbard, E. N. 1985, *Ap. J.*, **295**, 394.
Puget, J. L., Léger, A., and Boulanger, F. 1985, *Astr. Ap.*, **142**, L19.
Rees, M. J. 1984, *Ann. Rev. Astr. Ap.*, **22**, 471.
Rees, M. J., Silk, J. I., Werner, M. W., and Wickramasinghe, N. C. 1969, *Nature*, **223**, 788.
Reynolds, S. P., and McKee, C. F. 1980, *Ap. J.*, **239**, 893.
Rice, W., Lonsdale, C. J., Soifer, B. T., Neugebauer, G., Kopan, E. L., Lloyd, L. A., de Jong, T., and Habing, H. J. 1988, *Ap. J. Suppl.*, **68**, 91.
Rieke, G. H. 1985, in *Astrophysics of Active Galaxies and Quasi-stellar Objects*, ed. J. S. Miller, (Mill Valley, CA: University Science Books), p. 235.
Rieke, G. H., and Lebofsky, M. 1979, *Ann. Rev. Astr. Ap.*, **17**, 477.
———. 1981, *Ap. J.*, **250**, 87.
Robson, E. I., Gear, W. K., Brown, L. M. J., Courvoisier, T. J.-L., Smith, M. G., Griffin, M. J., and Blecha, A. 1986, *Nature*, **323**, 134.
Roche, P. F., and Aitken, D. K. 1985, *M.N.R.A.S.*, **213**, 789.
Roellig, T. L., Becklin, E. E., Impey, C. D., and Werner, M. W. 1986, *Ap. J.*, **304**, 646.
Sanders, D. B., Soifer, B. T., Elias, J. H., Madore, B. F., Matthews, K., Neugebauer, G., and Scoville, N. Z. 1988*a*, *Ap. J.*, **325**, 74.
Sanders, D. B., Soifer, B. T., Elias, J. H., Neugebauer, G., and Matthews, K. 1988*b*, *Ap. J. (Letters)*, **328**, L35.
Scheuer, P. A. G. 1987, in *Superluminal Radio Sources*, ed. J. A. Zensus and T. J. Pearson (Cambridge: Cambridge University Press), p. 104.
Schmidt, M., and Green, R. F. 1983, *Ap. J.*, **269**, 352.
Shakura, N. I., and Sunyaev, R. A. 1973, *Astr. Ap.*, **24**, 337.
Shields, G. A. 1978, *Nature*, **272**, 706.
Shuder, J. M., 1981, *Ap. J.*, **244**, 12.
Soifer, B. T., Sanders, D. B., Madore, B. F., Neugebauer, G., Danielson, G. E., Elias, J. H., Lonsdale, C. J., and Rice, W. L. 1987, *Ap. J.*, **320**, 238.
Soifer, B. T., Sanders, D. B., Neugebauer, G., Danielson, G. E., Lonsdale, C. J., Madore, B. F., and Persson, S. E. 1986, *Ap. J. (Letters)*, **303**, L41.
Tananbaum, H., Avni, Y., Green, R. F., Schmidt, M., and Zamorani, G. 1986, *Ap. J.*, **305**, 57.
Telesco, C. M., and Harper, D. A. 1980, *Ap. J.*, **235**, 392.
Treves, A., Bouchet, P., Chiappetti, L., Ciapi, A., Falomo, R., Maraschi, L., and Tanzi, E. G. 1988, preprint.
Unger, S. W., Pedlar, A., Axon, D. J., Whittle, D. M., Meurs, E. J. A., and Ward, M. J. 1987, *M.N.R.A.S.*, **228**, 671.
Usher, P. D. 1978, *Ap. J.*, **222**, 40.
Ward, M., Elvis, M., Fabbiano, G., Carleton, N. P., Wilner, S. P., Lawrence, A. 1987, *Ap. J.*, **315**, 74.
Wilkes, B. J., and Elvis, M. 1987, *Ap. J.*, **323**, 243.
Willner, S. P., Soifer, B. T., Russell, R. W., Joyce, R. R., and Gillett, F. C. 1977, *Ap. J. (Letters)*, **217**, L121.
Wilson, A. S., and Ulvestad, J. S. 1982, *Ap. J.*, **263**, 576.
Wright, E. L. 1987, *Ap. J.*, **320**, 818.
Young, E. T., Neugebauer, G., Kopan, E. L., Benson, R. D., Conrow, T. P., Rice, W. L., and Gregorich, D. T. 1985, preprint.
Young, J. S. 1987, in *IAU Symposium 115, Star Formation*, ed. M. Peimbert and J. Jungaku (Dordrecht: Reidel), p. 557.
Zdziarski, A. A. 1986, *Ap. J.*, **305**, 45.

K. MATTHEWS, G. NEUGEBAUER, D. B. SANDERS, and B. T. SOIFER: Downs Lab, 320-47, California Institute of Technology, Pasadena, CA 91125

E. S. PHINNEY: Theoretical Astrophysics, 130-33, California Institute of Technology, Pasadena, CA 91125